Literature review

Quasi-static and Dynamic pile load tests

- - - - - - - - N.Q.HUY - - - - - - - -

Table of contents:

I. Introduction

Pile testing, which plays an importance role in the field of deep foundation design, is performed by static and non-static methods to provide information about the following issues: (*Poulos, 1998*)

- The ultimate capacity of a single pile.
- The load-displacement behavior of a pile.
- The performance of a pile during the test conditions.
- The integrity of a pile (pile integrity test).

For the purposes of verification the design axial capacity and the static load – settlement behavior of piles, the static pile load test has long been considered as the most reliable method but because of its high cost and time consuming, non – static pile load tests are looked as efficient substitutions. The two non – static testing methods, i.e. dynamic and quasi – static pile load test are objects of this report.

The non – static pile load tests are performed by means of exerting an impact force on the pile head while measuring and recording the responses of the pile, from which the test results are determined. Duration of the impact force (T), longitudinal wave velocity of tested pile (c) and pile length (L) are used as key factors to classify the testing methods. For instance, the relative wave length $\Lambda = \frac{T.c}{2L}$ (*Holeyman, 1992*) or the wave number $N_w = \frac{T.c}{L}$ (*Middendorp et al., 1995*) or the relative duration $t_r = \frac{T}{\frac{2L}{c}}$ (*Karkee et al., 1997*) have been used. The Research Committee on Rapid Load Test Methods in Japan (1998) proposed the classification of pile load test methods as shown in figure 1. In which, the practical boundary between static and non-static testing method is $\Lambda = t_r = 500$ or $N_w = 1000$; while the boundary between dynamic and quasi – static pile load test is $\Lambda = t_r = 5$ or $N_w = 10$. Figure 1 also shows the dynamic effects to be taken into account in interpretation of load testing results.

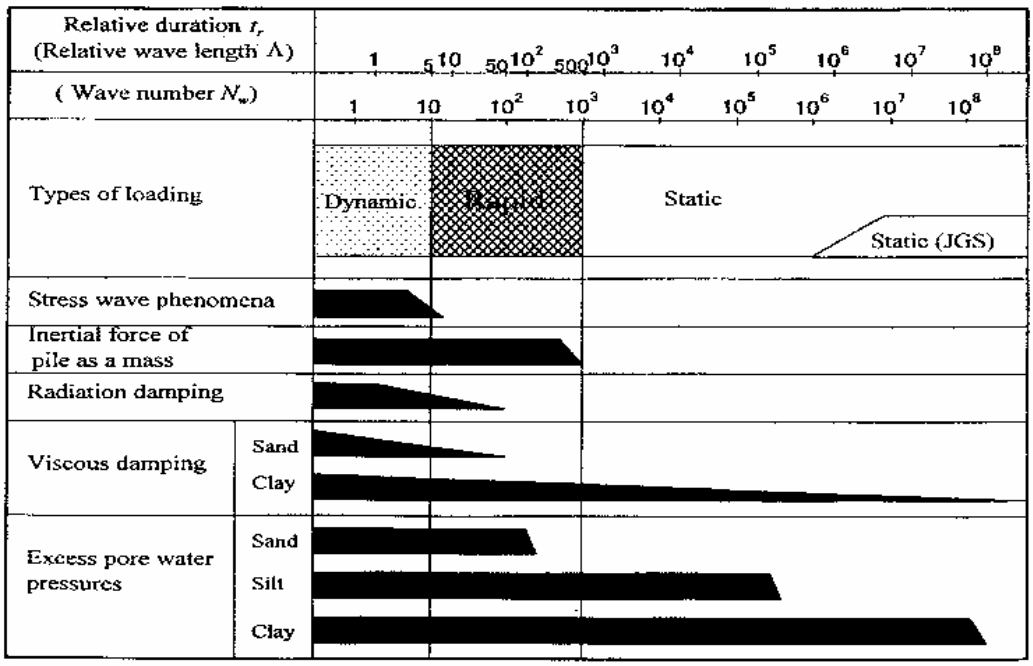

Figure 1: Classification of pile load test methods.

By review the published papers, firstly the quasi – static and dynamic pile load tests are presented with following aspects:

- The testing procedures.
- The interpretation methods and case histories.

Then, some problems that affect the interpretation results are discussed such as the stress wave phenomena, the rate effect, and the excess of pore water pressure.

Finally, some suggestions or further studies for improving the reliability of these non – static pile load tests are concluded.

II. Quasi-static testing methods

Quasi-static pile load test is a testing procedure with a relatively long duration of impact force, ranges from 100 to 200 milliseconds. In the loading method, if the impact force is developed by dropping a heavy mass, the testing method is correlative named Dynatest (*Gonin et al, 1984*) or Pseudo-static pile load test (*Schellingerhout et al, 1996*); if that by launching a reaction mass, the testing method is named as STATNAMIC pile load test (*Birmingham & Janes, 1989*). Although these tests are different in the way to create the impact force they are the same in the applied force vs. time manner. More details in each testing method will be discussed below. Generally the weight of falling mass or reaction mass is about 5%-10% of the intended maximum dynamic load on the test pile (*Middendorp et al, 1992*).

2.1. Quasi-static pile load test procedures

2.1.1: Dynatest and Pseudo-static pile load test

The Dynatest (*Gonin et al, 1984*) or Pseudo-static pile load test (*Schellingerhout et al, 1996*) is carried out by drop a heavy ram with a coiled spring to the head of the test pile. This creates a slow-rising and long-lasting impact force to pile head as theoretical calculated in figure 2. The coiled spring is attached to the pile head (in Dynatest) or to the bottom of the falling mass (in Pseudo-static test). The reduction of the coiled spring stiffness and increasing of drop mass is a feasible way to lengthen the duration of the impact force (*Holeyman, 1992*).

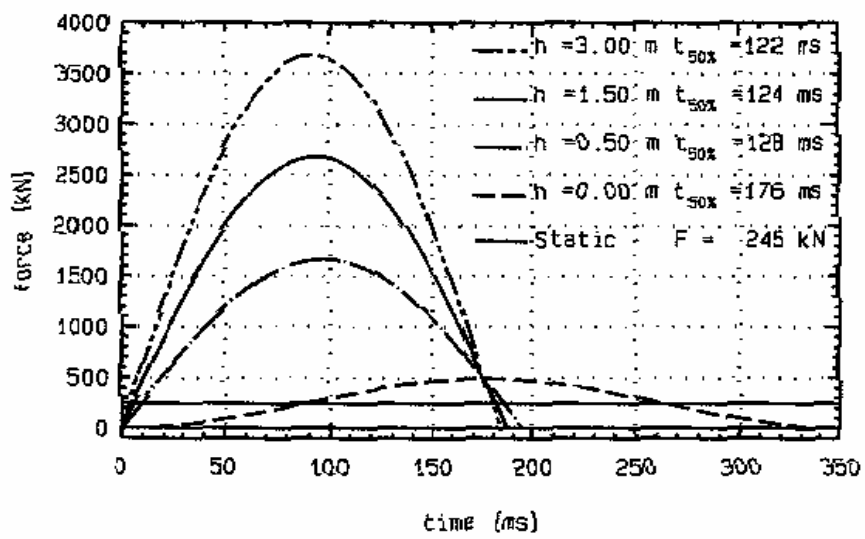

Figure 2: The force as a function of time for different drop heights.
(Schellingerhout et al, 1996)

The loading equipment is mounted on a small tracked vehicle, with a ram weight of 15-25 tons. The required measurements for the test are pile head force and displacement. The measurement devices for the test consist of a load cell and an optical displacement measuring device. The load cell that is placed on the pile top and optical displacement measuring device is placed at a distance of about 10m or more from the test pile to eliminate the influence of ground vibrations. When the pile head has been prepared, the rig is positioned, the measured devices are installed the test can start. First, the ram weight is lifted to a predetermined height vary from 0,1-1,4m by two jacks. Then a number of blows are executed to the pile by freely drop the ram from increasing heights (*Schellingerhout et al, 1998*). After impact to the pile head, the ram bounces and is picked up at its highest position by automatic catching system.

In good condition, 10 piles can be tested a day.

2.1.2: STATNAMIC pile load test

In 1989, Birmingham Corporation Limited (Canada) and TNO Building & Construction Research (The Netherlands) had jointly developed a so called STATNAMIC test, a new pile load testing method, with a specific testing device. This STATNAMIC test device consists of a pressure chamber, reaction mass and a catching system (*Janes et al, 1989*). The pressure chamber comprises of a piston and a cylinder is used to produce high pressure gases by burning of solid fuel for launching the reaction mass. As consequence, a reaction force pushes the pile downward. The reaction mass is a series of concrete or steel rings, whose weight is about 5-10% of total desired load to be applied to the test pile (*Middendorp et al., 1992*), so it is easily transported and installed. The catching system is gravel catching system or hydraulic catching mechanism, which is used to catch the reaction mass before it falls down on the pile head again.

Procedure to perform the STATNAMIC test is little different between two kinds of catching system but generally following these steps: prepare the pile head, place the testing device on the pile top, secure the reaction mass to the cylinder and start the test. The test is started by burning a volume of solid fuel in the pressure chamber, creating an increasing high pressure gases that push the reaction mass upward with the acceleration of about 20g while the equally opposite force pushes the pile downward. The downward velocity and acceleration of the pile are normally 0.5 - 1.0m/s and 1.0g – 3.0g, respectively. A typical load-time diagram is show in figure 3. The peak and duration of the applied force can be controlled by adjusting the weight of reaction mass, the volume of solid fuel or the characteristics of pressure chamber. During the test, the applied force is directly measured by a pressure transducer housed in the piston base, the pile head displacement is measured by use of laser sensor. Nowadays, the gravel catching system device gets the testing capacity up to 40 MN and can perform one test a day whereas that of hydraulic catching mechanism is 8 MN and 3 or 4 tests a day respectively (*Birmingham, 2000*).

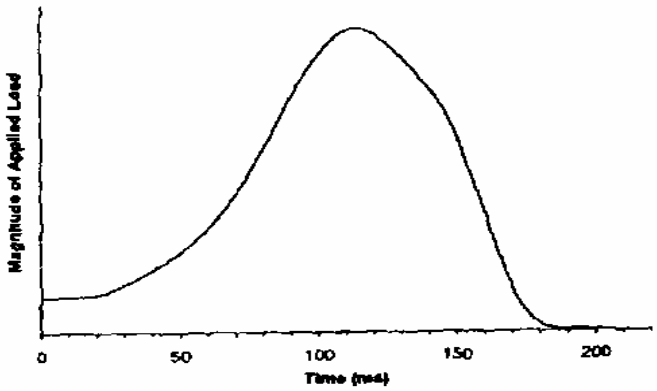

Figure 3: Typical STATNAMIC load-time diagram.

2.2. Data collections

2.2.1. Measurements

During the quasi-static pile load test event the indispensable collected data are applied load and displacement at pile head as a function of time. In addition, some more items such as acceleration at pile head and pile toe, velocity at pile head, axial strain of the pile are collected upon the testing aims, the interpretation methods, and the availability of measurement devices. The measurement data can be divided into two groups *(Holeyman –1992)*: dynamic measurements, which are force, pressure, stress, or strain; and kinematic measurements, which are displacement, velocity, and acceleration.

The applied force at the pile head is measured by a load cell, which is mounted directly between the loading device and the pile head. This device should be checked before the test for the accuracy (accurate to 0,1% - *Janes et al, 1991*) and rated capacity. Normally, the applied force at the pile head is derived from the compression of the coiled spring for Dynatest or measured by the pressure gauge fixed in the pressure chamber for STATNAMIC test.

The displacement at the pile head is measured by a special displacement transducer, which is capable of measuring displacements directly and continuously. The displacement transducer consists of a light sensitive cell placed at the central longitudinal axis of the pile and a remote laser light source stationed at a distance of 10m to 20m from the test pile to be not influenced by ground vibrations.

The pile head acceleration is measured by a acceleration transducer, which is attached as near the central longitudinal axis of the pile as possible. The accelerometer shall appreciate for the test and the bias shall not exceed 0,03g (*draft of ASTM standard, 1998*).

2.2.2. Data recording

All measurement devices are connected to the analog or digital or both recording system. The data acquisition system should be capable of acquiring a recorded signal with a minimum of 50ms of pre-event data and 150ms of post-event data. Data sampling frequency should be 1 kHz or more. The collected signals are prepared in the diagram form of measured items versus time or applied force versus displacement of pile head and be displayed in graphical or numerical mode.

2.3. The interpretation of result and case histories

2.3.1: Interpretation methods

In this section, three common used analytical interpretation methods for estimate a pile's static load – displacement behavior are presented. They are concentrated mass model analysis, one-dimensional stress wave analysis and finite element method.

1) The concentrated mass model analysis

- This method is first proposed for STATNAMIC test by *Middendorp et al, 1992* and known as Unloading point method (UPM). The concentrated mass model is in figure 4.

In this method to determine the static load-displacement curve, *Middendorp et al (1992)* supposed the pile as a rigid body so that the velocity of the pile during the test is synchronized. The forces acting on the pile during a STATNAMIC test and a STATNAMIC load vs. pile head displacement diagram show in figure 5.

Equilibrium equation for pile mass:

$$F_{stat} = F_{soil} + F_a = F_u + F_v + F_p + F_a \qquad (1)$$

Where:

F_{stat} : applied STATNAMIC load – measured

F_a : Inertial force of the pile mass, $F_a = M_{pile} . a(t)$, with M_{pile} is the total mass of the pile and a(t) is measured acceleration of pile head.

F_{soil} : soil resistance of pile shaft and toe, $F_{soil} = F_u + F_v + F_p$, which is composed of static resistance F_u , dynamic resistance F_v and water pore pressure force F_p.

$F_v = C_v . v(t)$, with C_v is a constant damping value; v(t) is measured velocity of the pile.

For simplification, the pore pressure is taken into account as a part of the damping force and supposed that linear to v(t). So that:

$(F_v + F_p) = (C_v + C_p). v(t) = C . v(t)$

From equation (1), we get:

$$F_u = F_{stat} - F_v - F_a = F_{stat} - C . v(t) - M_{pile} . a(t) \qquad (2)$$

All parameters on the right hand of equation (2) are known from measurement data except the damping coefficient (C) that will be determined by the Unloading point method. A STATNAMIC load – displacement curve in figure 5 is divided into 5 key parts and the damping coefficient is supposed unchanged in each part. Hereafter, the subscript number indicates the value at a time in that part number.

+ In part 1, the STATNAMIC reaction mass is placed on the pile top. The load displacement behavior is fully static. The measured load and displacement at the end of area 1 are called F_{stat} and u_{stat}. The spring stiffness k_1 in this area can be calculated as:

$$k_1 = F_{stat} / u_{stat}$$

+ In part 2, the reation mass is launched, STATNAMIC loading starts. The soil behavior is elastic. The assumption is the spring stiffness k_2 at the start of area 2 equals k_1 of area 1. The damping coefficient (C) the expressed as:

$$C_2 = (F_{stn2} - k_1.u_2 - m.a_2)/ v_2$$

+ In part 3, the damping and inertia force increase progressively; the maximum STATNAMIC load is reached at the end of this part. The static soil resistance reaches its ultimate strength and yields at a value F_{uy} .

+ In part 4, the STATNAMIC load decreases. Because of the inertia of the pile, the displacement is still increasing. At the end of this area, pile displacement reaches a maximum value u_{max} so the pile velocity becomes zero; the correlated time called t_{umax}. Due to the zero velocity, the damping force becomes zero and the STATNAMIC load minus the inertia force equals the static soil resistance at this point.

$$F_u(t_{umax}) = F_{stn}(t_{umax}) - m.a(t_{umax})$$

The value $F_u(t_{umax})$ is considered as maximum static soil resistance and equivalent to the yielding value F_{uy} , which is assumed to remain constant throughout area 4, $F_{uy} = F_u(t_{umax})$. The damping (C) at any time within part 4 as:

$$C_4 = (F_{stn4} - F_{uy} - m.a_4)/ v_4$$

Then assuming the damping coefficient (C) in part 3 and part 5 equivalent to the mean value of (C) in part 4, the static resistance F_u can be calculated in part 3 and 5 as:

$$F_u(t) = F_{stn}(t) - C_4.\, v(t) - m.a(t)$$

+ In part 5, the pile is unloading and the pile final settlement of the pile U_{set} reaches at the end.

Once the damping coefficient (C) is determined, the load – displacement diagram can be drawn representing the static soil resistance as function of displacement.

Because of rigid pile assumption, the Unloading point methd only gives good results for STATNAMIC cases that have the wave number N_w is larger than 12 (***Baldinelli, 1999***). In the cases the wave number N_w smaller than 12, the rigid pile assumption is not valid so the UPM can not apply. To overcome this obstacle, the Segmental unloading point method (SUPM) is proposed for the test with N_w smaller than 12 (***Justason, 2000***). The SUPM assumes the pile is divided into some smaller segments; each segment behaves as a mass of single degree of freedom. By embedded strain gauge to measuring the strain at different levels of the shaft, the applied STATNAMIC load on each segment can be determined and then the UPM can be applied to each segment.

- ***Kato et al. (1998)*** proposed another concentrated mass model that is capable of separating the shaft and toe resistance. The model is combined the shaft resistance model by ***Randolph and Simon (1986)*** and the toe resistance model by ***Randolph and Deeks (1992)*** as shown in figure 6. In this model, all parameters except shaft capacity (F) and toe capacity (Q_b) are initially assumed from the results of soil tests and soil investigations as:

Shaft resistance: $k_s = \frac{2.75G}{(\pi d)}$, $c_r = \frac{G}{V_S}$

Toe resistance: $k_b = \frac{8G}{\pi(1-n)d}$, $c_b = \frac{3.2G}{\pi(1-n)V_S}$

Additional mass at pile toe: $M_b = 2.d^3.\rho_s.\frac{0.1-n^4}{1-n}$

n : Poisson's ratio of soil; d: pile diameter

ρ_s : Soil density, $G = \rho_s.V_s^2$: shear modulus; V_s : shear wave velocity.

The measured STATNAMIC force is used as input in the analysis, the pile head displacement-time as out put. Matching between the out put and measured displacement-time is achieved by adjusting the soil shear modulus and capacity parameters (may be the shear strength). A static load – displacement behavior then derived from the using of identified soil parameters.

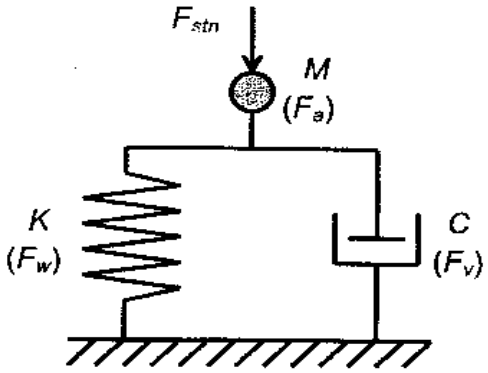

Fig 4: Concentrated mass model (P.Middendorp et al, 1992)

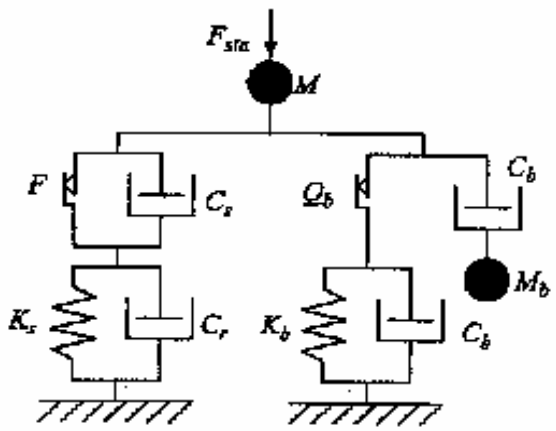

Fig 6: A new single mass model for statnamic test (K.Kato et al, 1998)

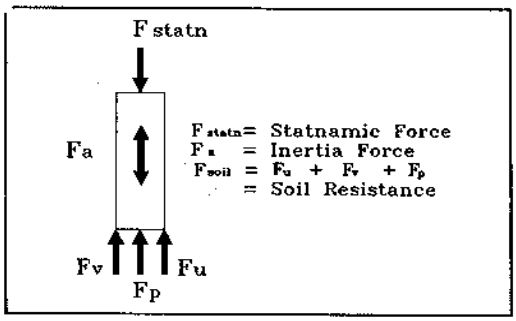

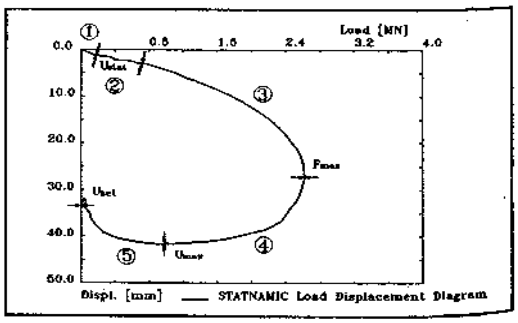

Fig 5: Force action on the pile and load-displacement diagram (P.Middendorp et al, 1992).

2) <u>One - dimensional stress wave analysis</u>

The application of one-dimensional stress-wave propagation analysis has been widely used for the interpretation of dynamic pile load test results since 1960s. *El.Naggar et al, (1992)* first proposed this analysis method to the STATNAMIC test. *Nishimura et al (1995), Ochiai et al (1996), Matsumoto et al (1996), Ochiai et al (1997), Asai et al (1998), van Foeken et al (2000)* confirmed that one-dimensional stress-wave analysis with automatic signal matching technique is applicable to interpret the STATNAMIC test results and estimate the static load-displacement behavior of tested pile.

In the application to interpret results of a STATNAMIC test the pile – soil model and analytical algorithm are the same with that to dynamic test and will be detailed in the dynamic part. The pile – soil model of *El Naggar et al, (1992)* is showed in figure 7.

In the usage of signal matching technique in the analysis the STATNAMIC test, the two suggested matching targets to make the wave matching more reliable and to assure the uniqueness of solution are the measured pile head displacement and pile forces F_{stat} if the burning of the fuel also modeled.

The one-dimensional stress-wave analysis is also executed by dedicated software on personal computer, such as CAPWAP program developed by GRL, USA or TNOWAVE program developed by TNO Building and Construction Research Organization, Netherlands. Each of these programs has its own pile – soil models and the input parameters but the application of signal matching techniques is similar.

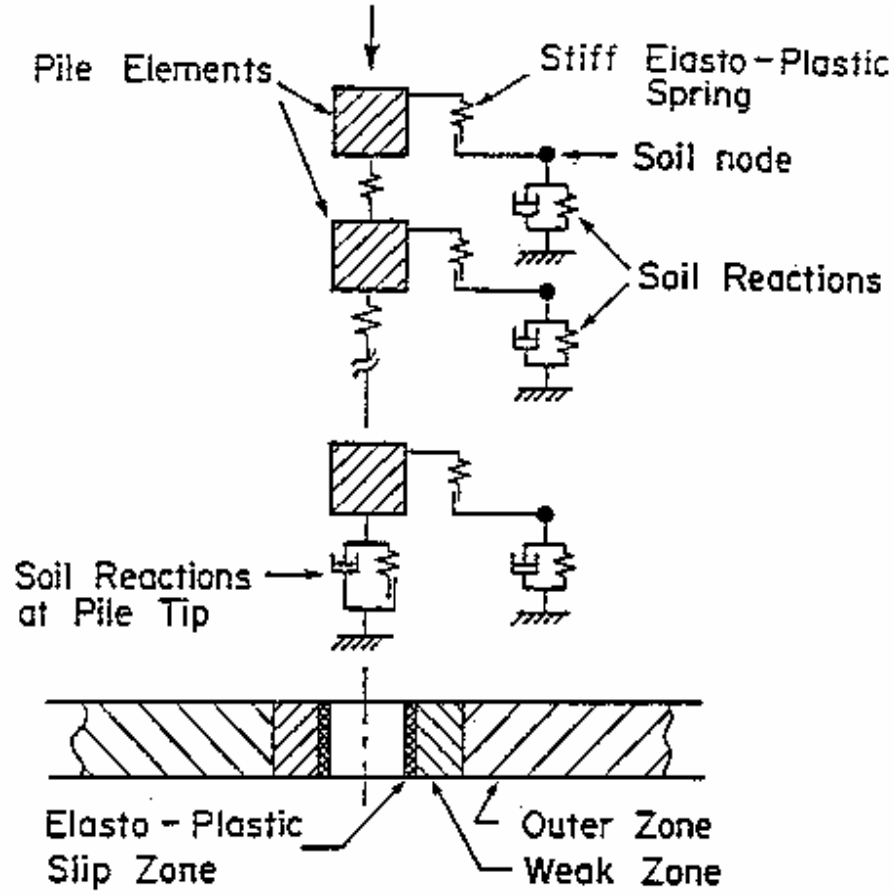

Figure 7: Pile – soil model (El.Naggar et al - 1992).

3) Dynamic finite element analysis

The finite element method with axi-symmetric model is applicable to analysis the axial STATNAMIC pile load test (*Matsumoto, 1998; Horikoshi et al., 1998*). In this model, joint elements are set along the pile shaft to take into account slip failure at the adjacent soil and pile shaft (figure 8). Linear elastic behavior was assumed for the soil response. The analytical sequence is shown in figure 9, which includes four steps: Soil investigation, STATNAMIC load test, analysis of STATNAMIC load test, and the final static pile analysis. The soil investigation step is to determine the analytical parameters, i.e. the soil physical and mechanic properties. Shear modulus value at small strain condition G_o was calculated from shear wave velocity V_s, which was estimated by P-S logging or the seismic cone penetration tests. The STATNAMIC pile head force is used as input to calculate the pile response in finite element analysis, i.e. pile head displacement – time or pile head velocity – time, to compare with a measured one. The shear modulus is reduced by multiplying with a reduction factor η ($\eta \leq 1$) to allow the effects of higher strain level on the soil responds. The dynamic analysis of STATNAMIC load test is iteratively conducted until the agreement between the calculated and observed pile behavior is matched in order to find the best reduction factor. At final step, the static pile behavior is analyzed with the best derived reduction factor.

The three-dimensional FEM is also used in analysis the STATNAMIC test, *Tsubakihara et al (1993, 1995); Yamashita et al (1994a, 1994b, 1995, 1998)*. But the 3D model is more adequate to STATNAMIC test on pile groups and lateral test rather than axial test because of the nature of problem and economic aspect.

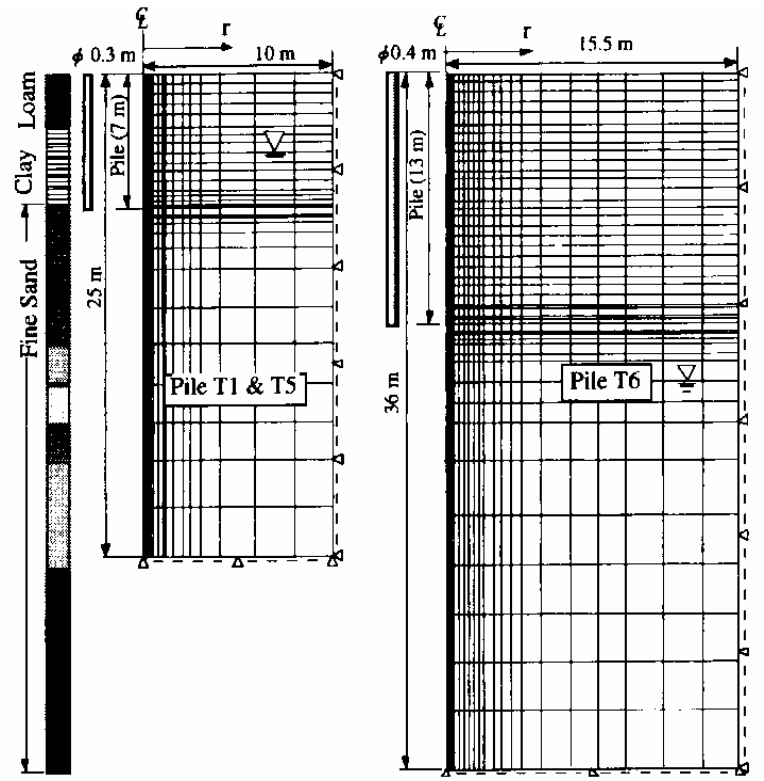

Fig 8: Finite element model (Horikoshi et al, 1998).

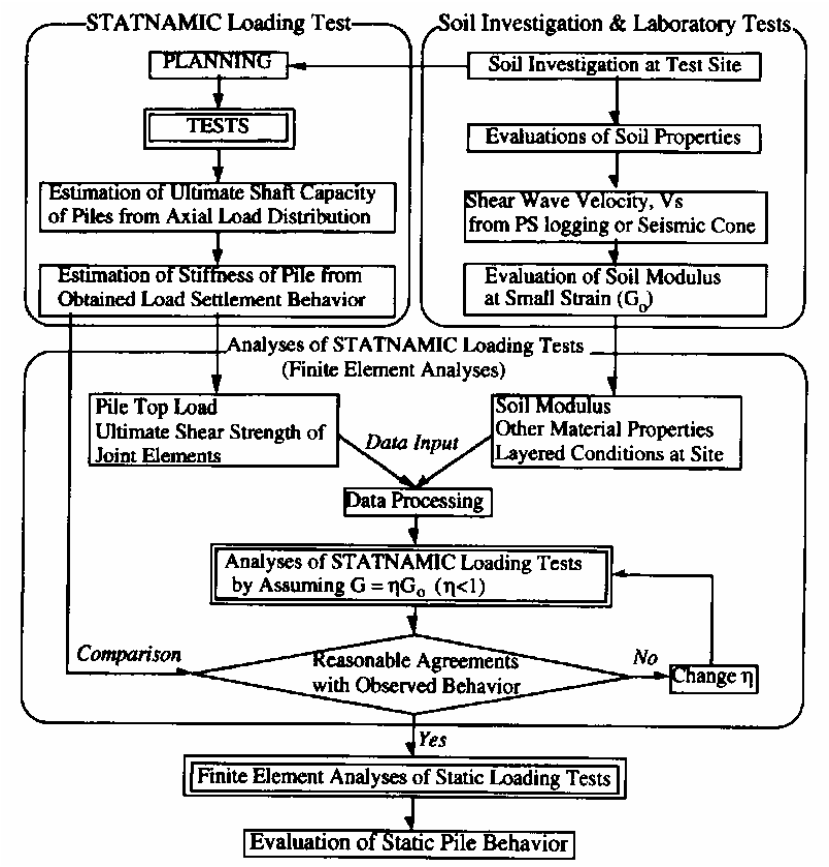

Fig 9: The finite element analytical sequence (Horikoshi et al, 1998).

2.3.2. Case histories:

All case histories are discussed here for the purpose of verification of above STATNAMIC interpretation methods.

1) Case history 1: the UPM method for interpret result of the STATNAMIC test on the Bayou Chico Bridge test site (*Justason et al, 1998*).

This case history details the applicability of the UPM on a 10.5m long, 600mm square prestressed concrete pile located at Pier 15 on the Bayou Chico Bridge in Pensacola, Florida. The site soil type is sandy soil. The STATNAMIC pile load test was performed by Berminghammer Foundation Equipment in January, 1997 one month after the static test. The goal of the test program was firstly, to confirm the design capacity of the pile and secondly, to compare the results obtained by the static test method and STATNAMIC test method (*Justason et al, 1998*). The STATNAMIC test was performed by a 14MN STATNAMIC device with a conventional gravel catching system. The design capacity of the pile was 1,3MN. The test pile was instrumented with vibrating wire and resistance strain gauges as well as an embedded toe accelerometer.

In this test, the applied load duration is 120ms , assuming the wave speed of 4000m/s, $N_w = \frac{T.c}{L} = 45,6$ so the damping constant as well as the test results can be determined by UPM method straightforward.

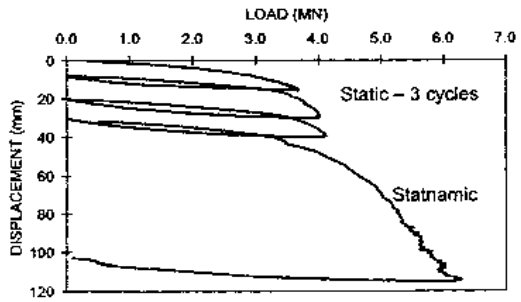

Fig 10: Static and STATNAMIC derived static load-displacement.

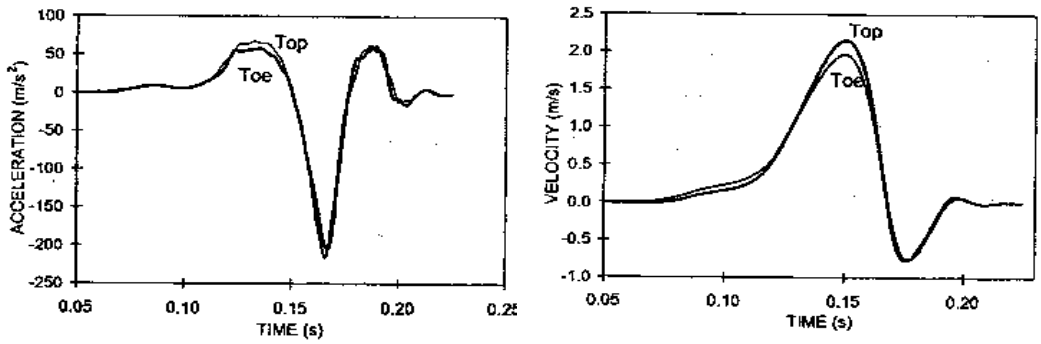

Fig 11: Acceleration and velocity vs. time of pile head and pile toe.

The results of the test show that:

- The test pile at Pier 15 achieved the required capacity based on the Davison failure load on both the static (3800 kN) and STATNAMIC (3300 kN) load tests.
- The static load-displacement curves derived from the STATNAMIC test from UPM method is similar to that of static test (figure 10).
- The similarity between the movement at the pile top and the pile toe (provided by the toe accelerometer) indicated that the pile essentially move as a rigid body (figure 11).

2) Case history 2: STATNAMIC test at the Keiji Bypass (*Maeda et al., 1998*).

The test pile is a cast-in-place concrete with 1.2m in diameter and 13.4m in length at the Mori Bridge of the Keiji Bypass southern part of Kyoto Pref. The soil profile is: filling soil up to GL-2m, alluvial clay up to GL-7m, alluvial gravel sand up to GL-12m, and diluvial gravel sand below GL-12.1m as a bearing layer.

The aims of the test are:

- Applicability of unloading point method (UPM) (including influences of excessive pore water pressure in the soil around the tip of pile).
- Applicability of signal matching analysis (SMA).
- Load – displacement relationship at the tip of pile.

For the above aims, the pile is installed strain gauges along the pile shaft, accelemeter on both ends; the pore water gauge in the soil around the pile tip (figure 12).

The static test employed in comparison results with STATNAMIC test (STN) is QM test (quick maintenance test) with maximum loading of 23.5 MN. It should be noticed that the QM test followed 6 cycles of SM tests (slow maintenance test) with maximum loading of 3.9; 7.8; 11.8; 15.7; 19.6; 23.5 MN. The STN test was performed a week after with the maximum STN load of 16 MN. The load – displacement diagram from STN and the QM static test are shown in figure 13. The figure revealed that during the STN test the soil's behavior was almost elastic, i.e. very small permanent displacement is observed. That was confirmed with the result from the static QM test that the total static capacity is about 17.7 MN (5.7 MN at pile shaft and 12 MN at pile toe). The stiffness during STN test is larger than that of static QM test, which may cause by the rate effect or set-up effect or both.

The excessive pore water pressure and STN loading vs. time are shown in figure 14. The pore pressure increased simultaneously with applied STN loading with the peak value at two positions 0.5m and 1.1m below the pile toe are nearly the same (80 kPa). The soil under the pile toe is not behavior in drained condition. The dissipation time is about 5 times longer than the loading duration, i.e. a consolidation process occurs in the soil, which may effect the real capacity of pile

- Results from UPM method

The static capacity is directly determined by the UPM method with and without the effect of excessive pore water pressure taken into account. The effect of excessive pore water pressure is simply evaluated by comparison between the pore pressure resistance (pore water pressure times with the pile toe's area) and the static resistance with total stress. The measured STN load (F_{stn}); the total soil resistance (F_{soil}); the derived static resistance with pore pressure (F_w) and without pore pressure ($F_{w'}$) vs. displacement are shown in figure 15. The results are:

Maximum static resistance without excessive pore water pressure: 17.52 MN

Maximum static resistance with excessive pore water pressure: 17.43 MN

Maximum pore water pressure resistance: 0.09 MN

The capacity derived from STN test seem close to that from SLT test, that confirmed the applicability of UPM method in bearing a pile capacity from STN test but very different in static load-displacement behavior of the pile. The stiffness of the derived curve is lower than that of measured curve. That may cause by the constant damping coefficient assumption (*Maeda et al., 1998*).

The pore pressure resistance is very small compared to the static pile capacity resulting in no significant difference between the derived capacities with and without excessive pore water pressure. However, the way that the authors took the excessive pore pressure into account seems over simplify. The examination of load – displacement characteristic at the pile toe will make it clear.

The UPM method was applied to the measurement in the pile toe. The STN pile toe force was obtained from re-bar stress transducers and the pile toe displacement was obtained from measurement of acceleration meters (*Maeda et al. 1998*). The measured STN load (F_{stn}); the measured static capacity; and the derived static resistance (F_w) vs. displacement at pile toe are shown in figure 16. It shows significant increase in stiffness and capacity from derived curve. At the same displacement correlates with maximum derived static resistance, the measured static capacity is 9 MN and the derived static capacity is 12 MN, i.e. the different is about 30%. It seems that the dynamic resistance is not fully removed from total resistance or others. The excessive of pore pressure will contribute in this increase because compressibility of water in undrained condition is very low. However, the difference between measured and derived capacity (3 MN) is very large compare to the simple pore pressure resistance (0.09 MN). The explanation for this problem is not clear at this moment and need further study.

- Results from SMA:

The pile – soil behavior during the STATNAMIC test was modeled as the model proposed by Randolph et al. (1992). The analysis was conducted in two cases:

- Case 1: the soil model's parameters such as spring stiffness and damping ratio are derived from seismic cone test; the yielding value is iteratively estimated for the best matching with displacement - time curve at the pile tip. The results (figure 17) showed much stiffer in pile-soil system and lower in pile capacity compare to SLT. *Maeda et al.,(1998)* explained this problem cause by a large value of spring stiffness derived from seismic cone test.

- Case 2: all model's parameters are determined from matching the displacement – time curve at the pile head. Results showed good agreement behavior but there are various kinds of soil parameters have to be optimized for fitting and hardly controlled. The static capacity from the SMA is 18.1 MN (5.9 MN on the shaft and 12.2 MN on the toe).

However, if we consider the load – displacement curve from SMA in figure 18 the matching is clearly not good in case 1 and can not said match during unloading phase in case 2. *Maeda et al., (1998*) did not give any reason for that but in my opinion, the reason is the soil behavior elastic during the STN test and not achieves failure so it is very difficult to define the yielding and quake values in the SMA. In addition, perhaps the excellent result from case 2 in figure 17 only achieve with the known result from static test in advance.

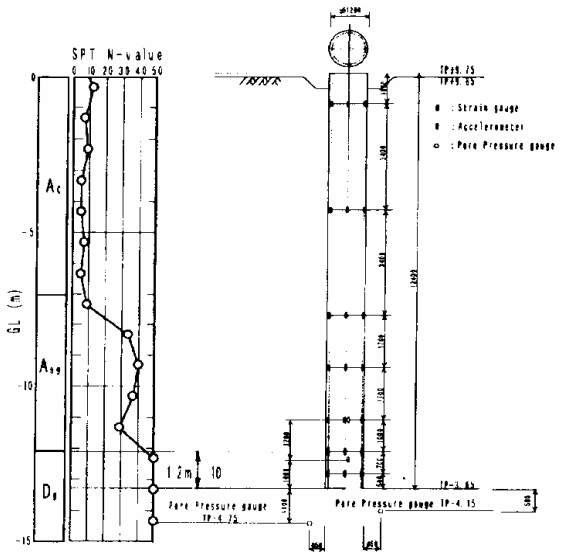

Fig. 12: Test pile and positions of measurement (Meada et al, 1998).

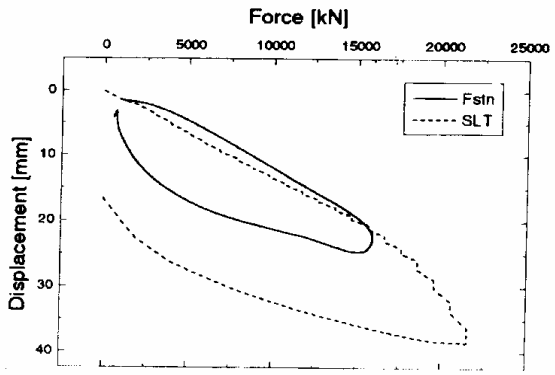

Fig. 13: Load-displacement relation (Meada et al, 1998).

3)

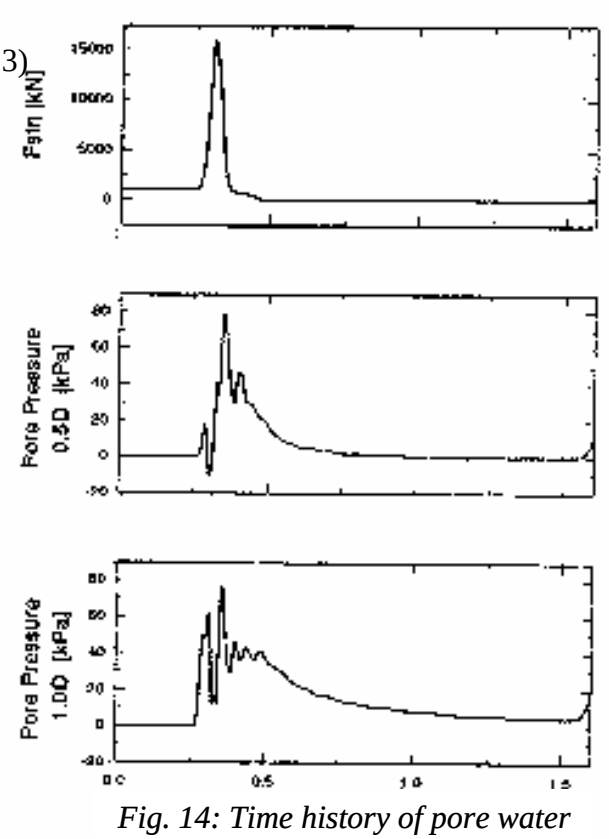

Fig. 14: Time history of pore water pressure (Meada et al, 1998).

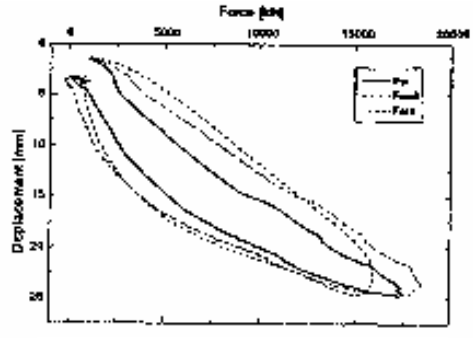

(*without pore water pressure*)

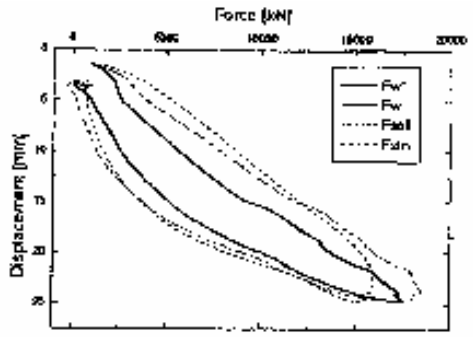

(*with pore water pressure)*

Fig. 15: Load-displacement relation. (Meada et al, 1998)

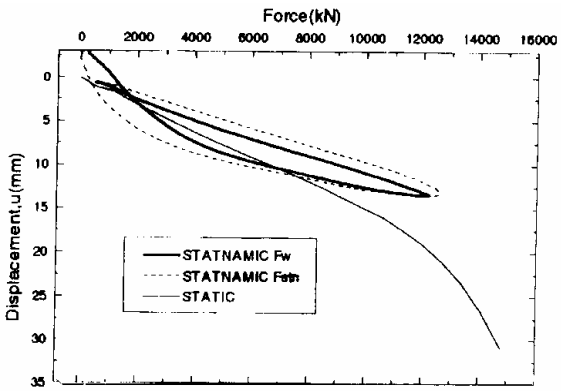

Fig. 16: Load-displacement comparison for SMA and SLT (Meada et al, 1998).

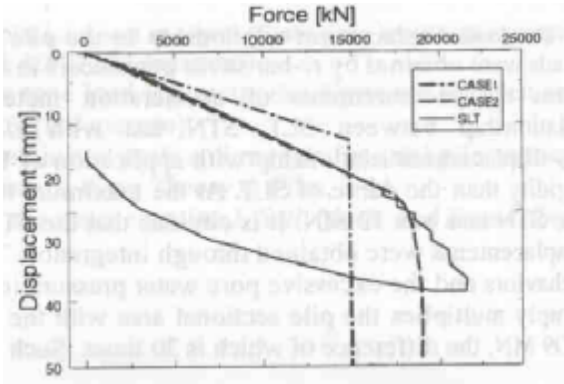

Fig. 17: Comparison between SMA and SLT (Meada et al, 1998).

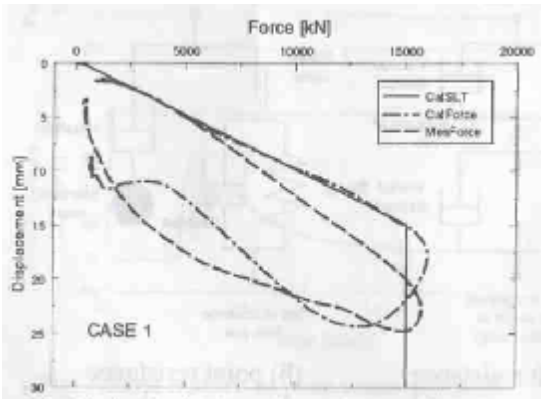

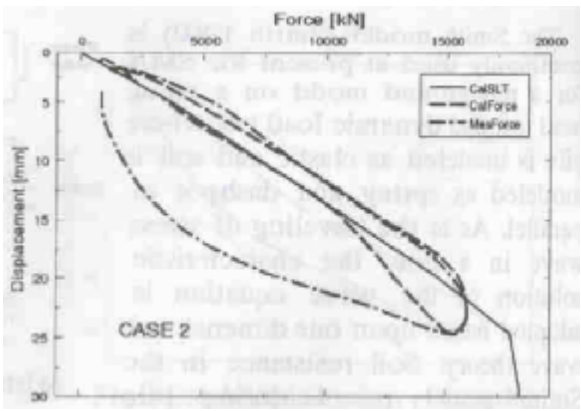

Fig. 18: Signal matching results (Meada et al, 1998).

3) Case history 3: FEM analysis of the STATNAMIC test piles at Shonan site in Chiba (*Hirokoshi et al, 1998*).

From 1994 to 1995, a number of static and STATNAMIC pile load tests were conducted at the Shonan test site in Chiba prefecture. Three piles T1, T5, T6 were re-analyzed using the dynamic finite element analysis. The test site soil profiles are shown in figure 19. The pile properties are shown in table 1.

Table 1. Dimensions of Test Piles

Property		Pile No.	
		T_1 to T_5 (in 1994)	T_6 (in 1995)
Type of pile		Prestressed high strength concrete pile	Open-ended steel pipe pile
Length	L (m)	7	13
Outer diameter	D_o (mm)	300	400
Inner diameter	D_i (mm)	180	382
Wall thickness	t_w (mm)	60	9
Cross-sectional area	A (cm^2)	452.4	110.6
Young's modulus	E (MN/m^2)	3.43×10^4	2.06×10^5
Mass density	r (ton/m^3)	2.6	7.85
Wave velocity	v_c (m/s)	3633	5123
Mass	M (ton)	0.823	1.58

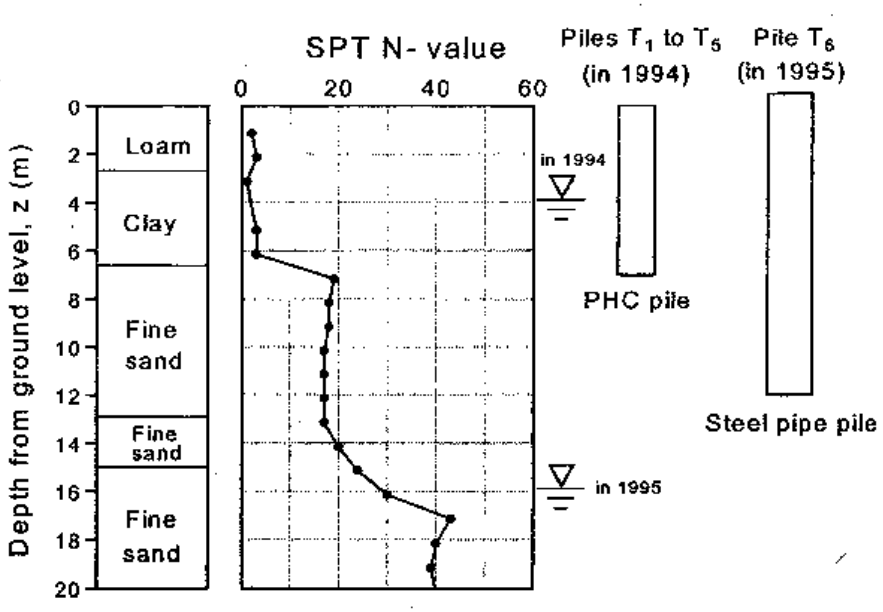

Fig 19: Soil profiles in Shonan test site (*Hirokoshi et al, 1998*).

The axi – symmetric finite element models are shown in figure 8. In this case, non-reflecting boundaries were set at on the side and the bottom boundaries of the model to avoid the effects of unnecessary reflection on the pile responses. The steel pipe pile T6 was replaced to an equivalent solid pile. The weight of the soil inside the pile was considered, but the soil modulus inside the pile was ignored for simplicity. For the determination of the analytical parameters, the results from the site investigation such as SPT (Standard Penetration Test) N value and the seismic cone penetration tests were used. The linear elastic model was assumed for the soil. Joint elements were set along the pile shaft to allow the slip response of the pile. Ultimate strength of the joint element in the loam and clay layers was estimated from the

measured distribution of axial force during the STN test. The stiffness of joint were set at high value so that the pile could not slip until the shear stress reaches the ultimate value, i.e. ≈ 85% of shear strength (*Hirokoshi et al, 1998*). The interface friction angle of 35 ^{o} and coefficient of earth pressure of 0.5 were assumed for the fine sand layer. The soil modulus at small strain condition G_0 was estimated first, and then the modulus was reduced by using a factor η (η ≤ 1) to allow the effect of higher strain level on the soil responses. The analysis in iterative manner with reducing of soil shear modulus is performed until reasonable match between measured and calculated pile head response. In order to see the effect of Poisson's ratio in the fine sand layer, it was set to 0.3 and 0.49 for the analysis case of pile T1 and T6.pile The reduction factor η = 0,4 was found to give good agreements between calculated and observed behavior of the pile head for pile T1, T5. That of pile T6 is η = 0,2. The static analysis is performed with the best reduction factor.

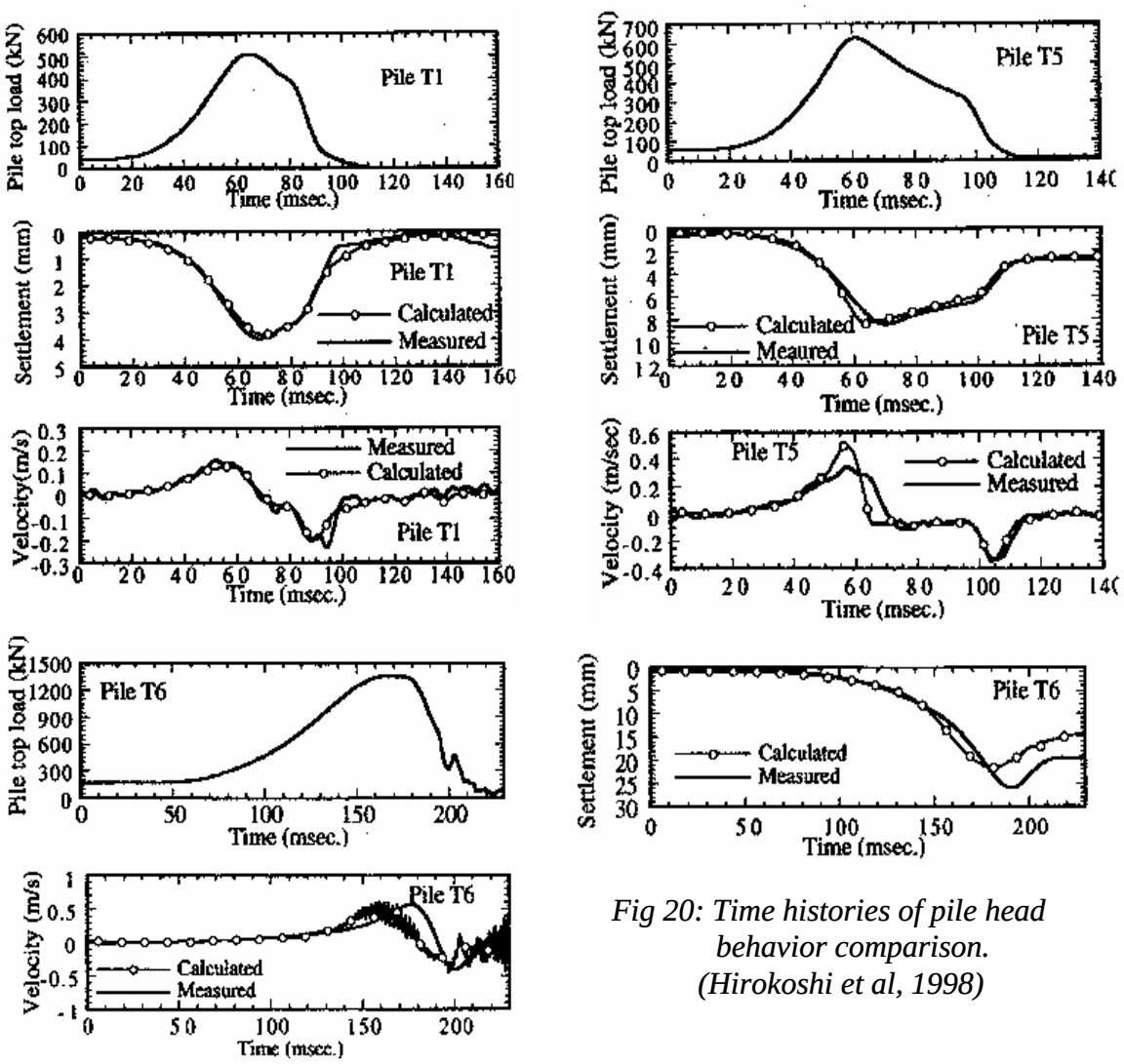

Fig 20: Time histories of pile head behavior comparison. (Hirokoshi et al, 1998)

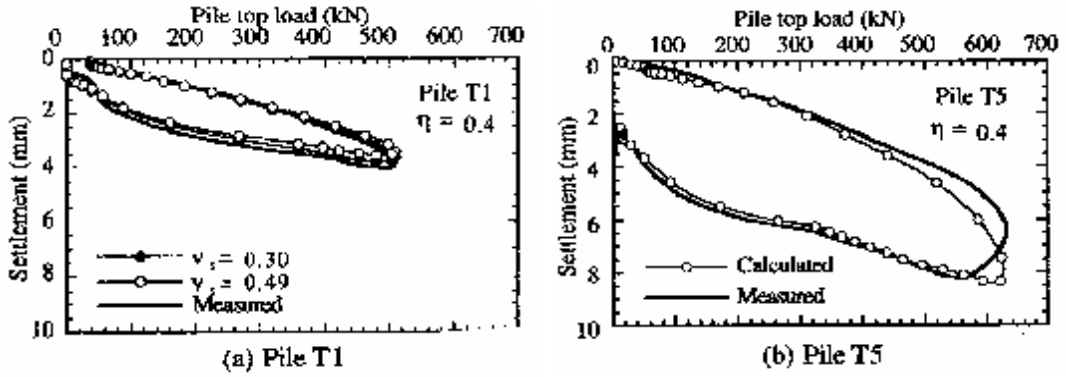

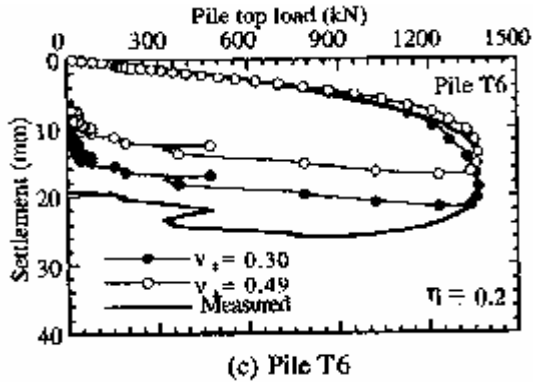

Fig 21: Load-displacement comparison. (Hirokoshi et al, 1998)

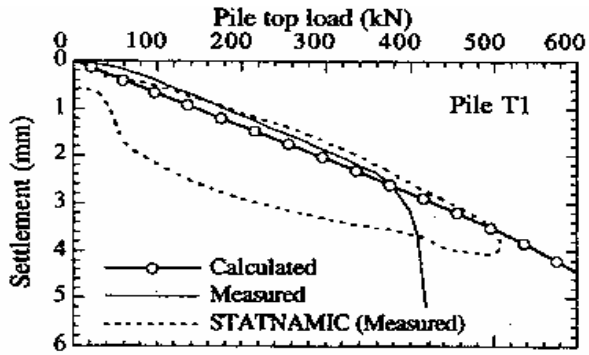

Fig 22: Estimated static loading behavior of pile T1 (Hirokoshi et al, 1998).

The time history of pile head responses are shown in figure 20. The load-displacement relations are shown in figure 21. The estimation static loading behavior of pile T1 is shown in figure 20. The following conclusions are drawn from the analysis:

- Although the soil model is linear elastic, the axi-symmetric FEM is proved a merit tool to analysis the STATNAMIC test results. The reasonable matching was achieved in all 3 cases The matching is much better in the cases the permanent displacement of the pile is small, i.e. may be the soil behavior elastic.

- A reasonable estimate of the initial pile stiffness is shown in using the soil parameters derived from the dynamic analysis for analyzing the static pile loading test but the ultimate pile resistance was not completely simulated because of the linear elastic model of the soil (fig.22). One can see from picture 21a that during the STN test, the permanent displacement of pile T1 is closely to zero, the soil is behavior elastic. It could be the reason for the good stiffness result in figure 22. Unfortunately, the pictures like picture 22 were not given for pile T5 and T6 where the permanent sets are bigger so the conclusion for this issue can not be made.

2.4. Discussion of the case histories

The above case histories show the application of interpretation methods for STATNAMIC pile load test. Consider the first two case histories, they are both concrete pile in sandy soil with the test order of SLT-STN and application of UPM method. The first case shows good correlation in load-displacement behavior but under predicted capacity (about 13%). The second case shows opposite results. It possibly causes by the true soil failure is not reach in the second STATNAMIC, which is needed to fully mobilize the soil resistance as remarked by *Janes et al. (1994)* and *Goble et al. (1995)* "*the test is clearly dynamic and must cause significant pile set after the test to be useful in ultimate "static" loads*". If the true failure in soil not reaches, the unloading point in the load-displacement diagram is only a virtual unloading point caused by the inertial of the pile rather than the unloading point defined by Middendorp et al, 1992 where the maximum static capacity is mobilized. It will cause the wrong result from the UPM method. Another problem related to the case history 2 is the excessive of pore water pressure. The simple evaluation of excessive pore pressure, measured pressure times pile area is not satisfy, the difference between calculated and measured static capacity compare to excessive pore pressure resistance is very large (30 times larger). In order to correctly facilitate the STATNAMIC pile load test in the pile engineer, the two problems should be solved but they are still questions at this moment. Perhaps a key for that lays in the basic understanding of soil behavior under the STATNAMIC loading condition.

The FEM analysis has been proved its applicability to analyze the STATNAMIC test cases but the linear soil model seems very crucial. It is not clearly modeling the failure in the static analysis and the matching is good in the STATNAMIC cases where the soil behavior elastic but not very good in the cases where the plastic deformation occur. More advance soil model is needed.

In order to verify the correlation between derived static capacity from STATNAMIC and static tests more case histories is taken from Mc. Vay et al. (2003) to examine. All cases are the successful STATNAMIC tests (true soil failure is reached) and in more or less in the same pile. The data is presented in table 2 and figure 23.

No.	Location	Pile type	Soil type	Test order	Static test kN	STN test kN
1	Noto, JPN	Steel pipe	soft rock	STL - STN	4380	5087
2	BC pier 5, USA	Driven PC	sand	STN - STL	3500	3957
3	BC pier 10, USA	Driven PC	sand	STL - STN	3380	5000
4	BC pier 15, USA	Driven PC	sand	STL - STN	3820	3322
5	Shonan T5, JPN	Driven bored	sand	STL - STN	446	489
6	Shonan T6, JPN	Driven pipe	sand	STN - STL	1100	1042
7	Contraband T114, USA	Driven PC	clay	STN - STL	1830	3070
8	Nia TP 5&6B, USA	Pipe	clay	STL - STN	2190	2600
9	Amherst 2, USA	Driven steel	clay	next	1214	1244
10	Amherst 4, USA	Driven steel	clay	next	965	1617
11	S9004 T1, CAN	AC	sand	next	1310	1350
12	S9102 T2, CAN	Pipe	clay	next	1040	2550

13	S9209 T1, USA	Driven steel	sand	STL - STN	7130	6370
14	S9306 T2, USA	Pipe	clay	next	1360	892
15	YKN - 5, JPN	Driven PC	sand	STL - STN	2770	2700
16	Hasaki - 6, JPN	Pipe	sand	STL - STN	1890	1490

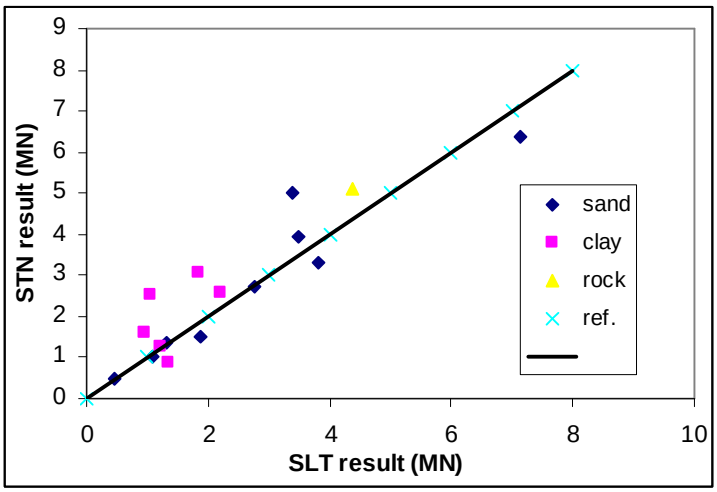

Fig. 23: Static capacity correlation.

From figure 23, the correlation between STANAMIC and static pile load test can be seen:

- In clay soil, the derived static capacity from STATNAMIC test is not much reliable and often over-predicted.
- In sandy soil, good correlation in low capacity piles but some scatter results appear for larger capacity piles.

It show that, at the knowledge of this, the STATNAMIC pile load test is only a good testing method for the static capacity of the pile in sandy soil if the successful test is achieved. Unfortunately, it is not easy to determine which is a apply STATNAMIC force for successful tests so the interpretation procedure for non successful cases are required. It may relate to the rate effect in elastic range.

III. Dynamic pile load test method

Dynamic pile load test (or high-strain dynamic testing) for bearing capacity of pile has been used for centuries. Most common test has the duration of impact force between 5 and 20 milliseconds, which is resulted from a dropping mass with a weight equal to 1%-2% of pile ultimate capacity (Holeyman, 1992). Before the 1950's, the only available mean of bearing the pile capacity from a "measurement" of set per blow is the dynamic formulae, which is now considered unreliable (*Hannigan et al.1996*). Since 1950's, the wave equation analysis with the help of digital computers and modern electronic measurements have been developed to retrieve more accurate results in estimating capacity and driveability. This part of report will deal with the dynamic testing method as from 1950s.

3.1. Dynamic pile load test procedures

Dynamic pile load test are performed by dropping a heavy mass on the cushioned pile head, which is monitored during the impact to obtain force and velocity as functions of time. The test can be carried out either at the end of driving (EOD – for driven pile) or restrike (for all types of pile). But because of the soil "set-up" and "relaxation" phenomena (Likins et al. 2000), the restrike tests, the test after the pile installed for sufficient wait time, usually give

more accurate axial static capacity result. A dynamic testing procedure usually includes the following steps.

1) Choosing the driving equipments

The driving equipments consist of hammer, hammer cushions, pile cushions and helmets. Choosing proper equipments (includes the hammer weight, the hammer drop height and the cushion details) is essential for a successful dynamic pile load test. Underpowered equipments will cause excessive numbers of hammer blows as well as under activated pile capacity. On the other hand, overpowered equipment may damage the pile and cause more expenses (Rausche, 2000). Hammer weight, drop height, and cushions details should be chosen so that hammer impact causes sufficient pile movement to mobilize the total soil resistance, and to assure that dynamic stresses in the pile will not damage its structural integrity. This is now well-done by pile driving simulation software (e.g. GRLWEAP or TNOWAVE). The pre-analysis for cast-in-place shafts withdraws following results (Hussein et al, 1990):

- Hammer weights equal to 1.4 to 1.6% of soil static resistance values.

- Drop heights corresponding to 7, 8, 9 and 10% of shaft lengths for shaft diameter sizes 1500, 1250, 1000 and 750 mm, respectively (minimum value of 2 m).

- Cushion thicknesses (t) equal to (L^2/2D) for a pile length (L) less than or equal to 30 m or (L^2/2D + 150) for L greater than 30 m where (t) is in mm and (L) in m (minimum value of 100 mm).

2) Executing a test

To the state-of-the-art development, all dynamic testing process is monitored on-site by PDA (Pile Driving Analyzer) system, a data acquisition system. For starting a test, it is necessary to excavate the soil around the test pile because the transducers are installed about 1,5 – 2 pile diameters from the pile head. The excavation is about 1,5 meters deep and wide enough for comfortable attachment of the transducers. Two pairs of strain and accelemeter transducers are attached to the two opposite side of the pile near the pile head. On pre-cast concrete piles, the transducers are connected to the pile with anchor bolts. On steel piles, the transducers are bolted to the pile by threaded holes or welded mounting blocks. All transducers are connected to PDA system and recovered after the test.

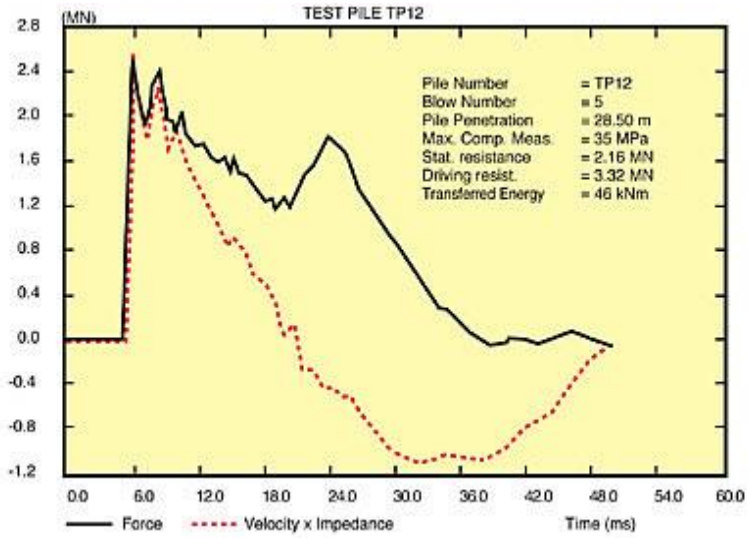

Figure 24: Typical PDA measured signal.

Initially, one or more blows with small drop height are given for purposes of signal checking and wave-speed verification. If the checking is satisfactory, the test is started with

increasing drop heights until either the set per blow exceeds a value sufficient to insure the full capacity activation or until the indicated capacity is above the required ultimate capacity, or until the stress become too large and the risk of pile damage is then too high. All testing data are automatically recorded on the hard disk by the PDA system for further analysis in office and report.

3.2. Data collections

3.2.1. Measurements

In the dynamic pile load test, the required measurement data are impact force and velocity at pile head as function of time.

Most commonly, the applied pile head load is derived from the measurement of strain at the pile head by strain transducers. In a few cases, a dynamometer is used to monitor the impact force during dynamic test .

Motion of the pile can be monitored by accelerometers, velocity transducers or displacement transducers. Accelerometers are widely used to monitor the pile head movement under the impact. Velocity, which is the most desirable format for interpretation, is obtained by direct integration of the accelerogram over time.

3.2.2. Data recording

In modern test, all testing measurement signals are recorded in digital computer. To avoid missing signal, the sampling rates for each measurement channel is ranged from 20 to 200 kHz. Retrieved data are stored in the numerical and/or diagram form.

3.3. The interpretation of result and case histories

Observations made and measurements collected during a dynamic test are used to estimate static bearing capacity of piles in difference ways. Most common and state-of-the-art interpretation methods are one – dimensional stress wave and finite elements analysis.

4.3.1. One – dimensional stress wave analysis:

The basis one – dimensional wave equation is given:

$$u(x,t)_{tt} = c^2 \cdot u(x,t)_{xx} \qquad (1)$$

Where:

u(x,t) : displacement as a function of distance and time

c : speed of wave propagate in pile; $c = \sqrt{\frac{E}{\rho}}$, with E and ρ are Young's modulus and the volumetric mass, respectively, of the pile material.

The general solution of eq. 1 is given by the method of characteristics in the form of:

$$u = f(x-ct) + g(x+ct) \qquad (2)$$

Where f, g are arbitrary functions, describe moving downward wave (f) and moving upward wave (g) with propagation velocity c. Such waves will travel unchanged in the pile unless a soil resistance is not exist or no change in pile impedance.

In the case of pile embedded in soil, the resistance of surrounding soil must be consider, the Eq. 1 becomes:

$$u(x,t)_{tt} = c^2 \cdot u(x,t)_{xx} \pm R_{tot} \qquad (3)$$

Where R_{tot} is total soil resistance. If a resistance force, such as shaft friction, appear at some point along the pile a tension and a compression stress will be induced on opposite sides of the point, causing two waves travel in opposite direction from the force. The upward wave will be felt at some time after the impact at the measuring point. So the recorded data can represent the behavior of pile.

Eq. (3) can be solved analytically or numerically but because of the complications involved in practical piling problems so the numerical solutions are predominance. Analytical solutions can be found details in literatures (Don Warrington, 1999). The close form of characteristic solution has been used to evaluate the resistance during dynamic test in signal processing procedure (see Signal processing). For more accuracy in predict static behavior of pile from dynamic test, the numerical solution is resorted (see Numerical solution).

1) Signal processing:

The collected signals are processed based on close form characteristic solution by simple operations such as addition and subtraction of simultaneous or phase – delayed signals for the purpose of evaluation the shaft, toe and total soil resistance. There are some signal processing methods available: Case method, Impedance method, TNO method (*van Foeken et al, 1996*). In these methods, the soil model is simple representing by a spring and a dashpot and the soil resistance is assumed only acting at the pile toe and/or at one point on pile shaft (figure 25).

Firstly, the total soil resistance mobilized by a hammer blow is calculated. When an impact wave introduces to the pile top at a certain time t (input), after a period of 2L/c part of the wave can be observed at top of the pile (out put). The reduction of the wave during the period of 2L/c, in which the wave travels through the pile and activates the soil resistance and turns back to the pile head, is called dynamic resistance. The dynamic resistance is calculated as sum of the downward traveling force at time t_{max} and the upward traveling force at time t_{max} + 2L/c (figure 26):

$$R_{tot} = F\downarrow(t_{max}) + F\uparrow(t_{max} + 2L/c) \qquad (4)$$

With F and v are measured independently; Z = ρ.c.A is pile impedance, the wave F↓ and F↑ can be determined:

$$F\uparrow = (F - Z.v)/2 \quad ; \quad F\downarrow = (F + Z.v)/2 \qquad (5)$$

The explanation for equation 5 & 6 is given in Appendix A.

The dynamic resistance here is the total soil resistance mobilized by a specific impact force and assumed to be the sum of static resistance R_s (displacement dependent component) and damping resistance R_d (velocity dependent component):

$$R_{tot} = R_s + R_d \qquad (6)$$

The static and dynamic components are then separated from total soil resistance by following procedures.

- Case method:

This is the first signal processing procedure for the pile capacity determination, which was developed at Case Institute of Technology (Goble et al, 1980). The total soil resistance is assumed to be concentrated at pile toe and the damping resistance is proportional to the maximum velocity of pile toe, i.e. $R_d = J_c.Z.v_{toe}$, so:

$$R_{tot} = F\downarrow(t_{max}) + F\uparrow(t_{max} + 2L/c) = R_s + R_d = R_s + J_c.Z.v_{toe}$$

$$v_{toe} = \frac{2.v(t_{max}).Z - R_{tot}}{Z} \qquad \text{(see Appendix A)}$$

$$R_s = R_{tot} - J_c . (2.v(t_{max}).Z - R_{tot})$$

The Case damping constant, J_c, is a nondimensional empirical and soil type dependent factor. J_c can be chosen based on pile load test database or more accurately by the basis of a correlation with a static load test or a signal matching technique.

- Impedance method:

In this method, the total shaft (S_{tot}) is assumed to concentrate at a point in the shaft and equal to the static shaft resistance. Only the total toe resistance (T_{tot}) is composed of static resistance (T_s) and dynamic resistance (T_d). The shaft resistance is equal to the maximum value of the upward traveling wave force in the time domain from t_{max} to t_{max}+2L/c:

$S_{tot} = S_{stat} = 2.F\uparrow (\max (t_{max} , t_{max}+2L/c))$ (see Appendix A)

The toe resistance is determined by:

$$T_{tot} = R_{tot} - S_{tot} = T_s . (1+ J_s.v_{toe})$$

$$T_s = \frac{T_{tot}}{(1+ J_s.v_{toe})}$$

Where: J_c is the Smith damping constant; v_{toe} is calculated from measured signal as in Case method.

- TNO method:

TNO method suppose that the total dynamic resistance R_{tot} composed of a shaft dynamic resistance S_{tot} concentrates at one certain point along the pile shaft and toe dynamic resistance T_{tot} and calculated as.

$$S_{tot} = S_s + S_d = 2.F\uparrow (\max (t_{max} , t_{max}+2L/c))$$

$$T_{tot} = T_s + T_d = R_{tot} – S_{tot}$$

The damping shaft resistance is calculated by: $S_d = v_{shaft} . C_{shaft}$

The damping toe resistance is calculated by: $T_d = v_{toe} . C_{toe}$

The average shaft velocity: $v_{shaft} = \frac{1}{Z} . (F(0,t_1)\downarrow - ½ .W)$ (see Appendix A)

The average toe velocity: $v_{toe} = \frac{1}{Z} . (2.F(0,t_1)\downarrow - W - P)$ (see Appendix A)

The damping parameters C_{shaft} and C_{toe} are calculated on the use of a static test or signal matching dynamic test in the same test site as reference. If a static case is used as reference, the static test must be instrumented to measure the static toe resistance.

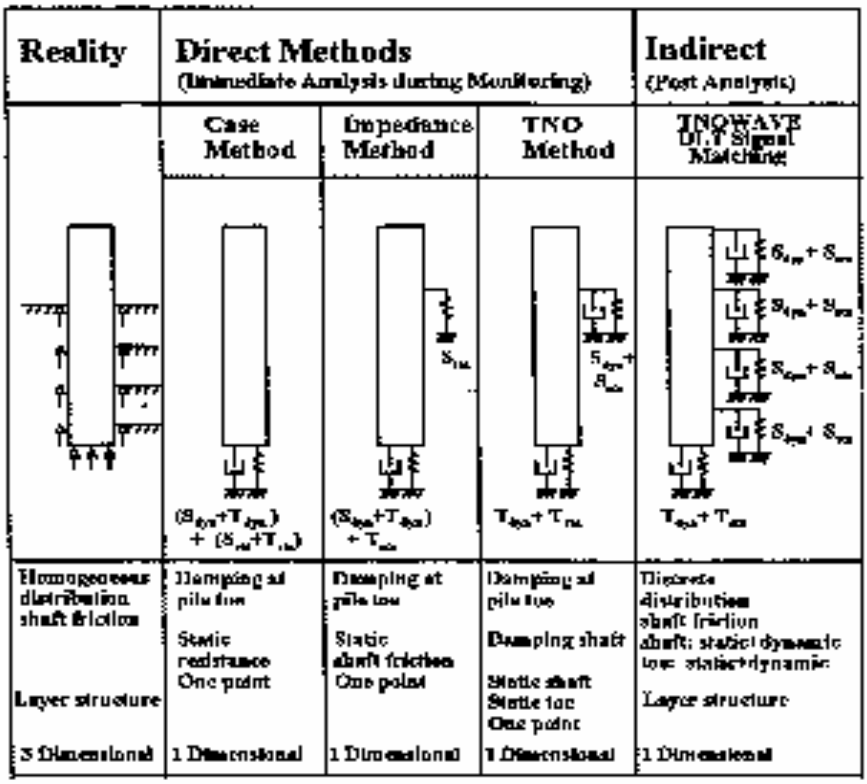

Figure 25: Idealize models in direct and indirect method.

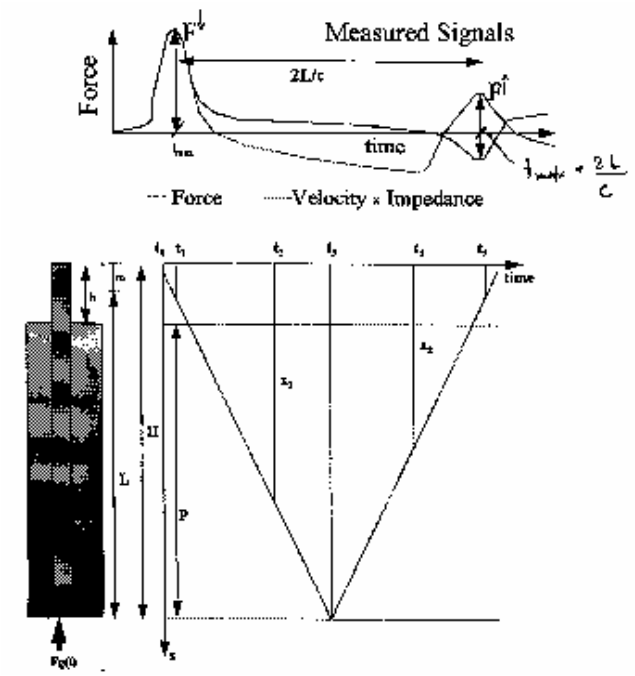

Figure 26: Quantities definition in signal processing method (van Foeken et al, 1996).

2) Numerical solution:

The essence of this method is an iterative calculation procedure (signal matching procedure) to achieve the matching between measured and calculated pile – soil system behavior, from that soil resistance parameters will be determined. The first practical numerical model was introduced by Smith (1960) based on the finite-difference method. Up to date, many improvements have been made to model the pile – soil behaviors more accurate during a

hammer blow. Up to date the one-dimensional method of characteristic method is widely accepted and applied. A number of computer programs have been developed based on method of characteristic together with iterative process to model the pile behavior such as CAPWAP (Rausche et al., 1985), TNOWAVE (Middendorp et al., 1987), and SIMBAT (Paquet, 1988).

In these analysis programs, the particular soil models may vary but the signal matching procedure is similar. From the measured strain and acceleration signal, pile top force and velocity are determined. Most common, the pile top force is used as an input to calculate the behaviors of pile – soil model. The output velocity is compared with the measured velocity. The soil resistance parameters are adjusted iteratively until the best match between calculated and measured behavior is archived. A static analysis is performed afterward using these soil resistance parameters to predict the static pile behavior. The process is illustrated in figure 26.

2-1) Pile-soil system modeling:

In Smith's model, the pile is divided into a sequence of concentrated masses separated by linear springs representing the material stiffness of the pile. The soil resistance acting on each mass is represented by a linear spring-slider for elasto – plastic static soil behavior in parallel with a viscous damper for velocity – dependent soil resistance (figure 27 & 28). There are some others more complicated models have been developed to describe "more accurate" the response of the system. Most remarkable is the work of Mitwally and Novak (1988), Randolph and Deeks (1992). In Mitwally and Novak model, the shaft and toe resistance are treated separately; the motion of the soil adjacent to the pile shaft is traced independently from that of the pile by adding an extra massless point at each pile segment (figure 7). Further more, Randolph and Deeks traced the motion of the soil under pile toe by adding a lumped mass at pile toe segment (figure 29). The characteristics of a driving system, i.e. ram, caplock, pile cap cushion springs, is simply taken to be linear (figure 27a). The characteristics of the soil components (figure 28) in models are considered subsequently.

In the method of characteristic, the pile is divided into equally spaced intersections. The soil resistance acts at interactions so between the interactions the pile is frictionless, a wave will propagate undisturbed. When a wave arrives at certain intersection apart of the wave will transmit and another part will reflect. The magnitude of transmit and reflect waves depends on the soil resistance at the intersection in the same manner as presented in Appendix A. The soil resistance is model similar in Smith's model.

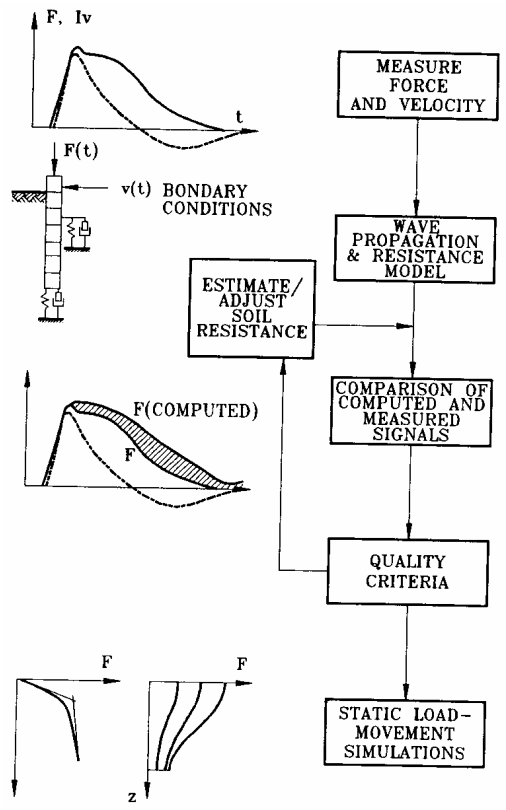

Figure26: Numerical analysis procedure (A.E. Holeyman, 1992).

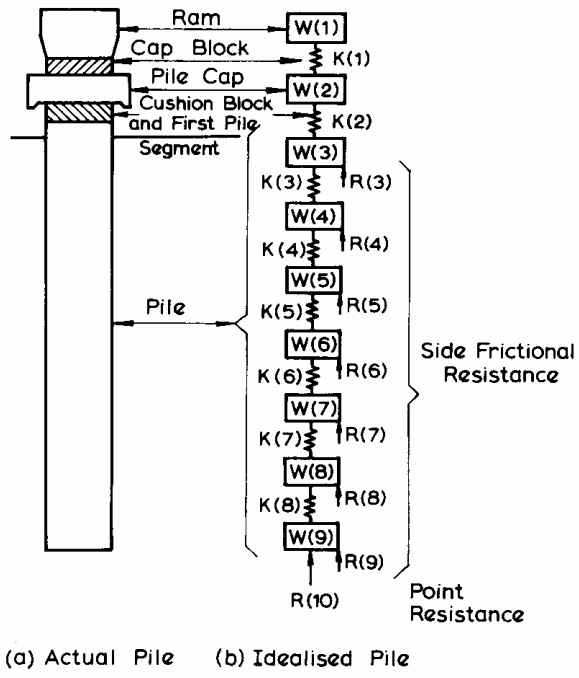

Figure 27: Idealization of pile (E.A.L. Smith, 1960)

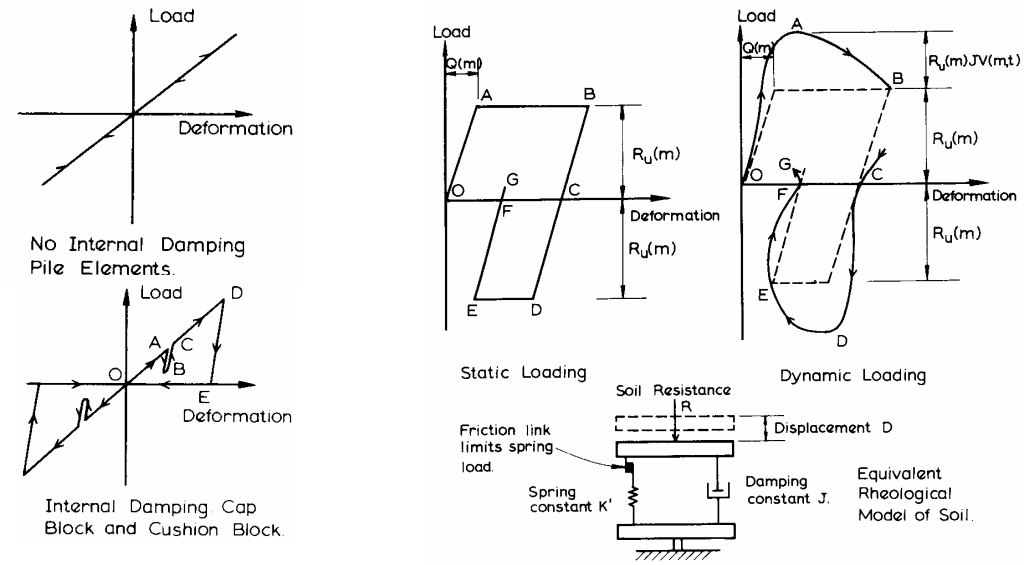

Figure 28: Load-deformation characteristics for pile and soil. (A.E.L. Smith – 1960)

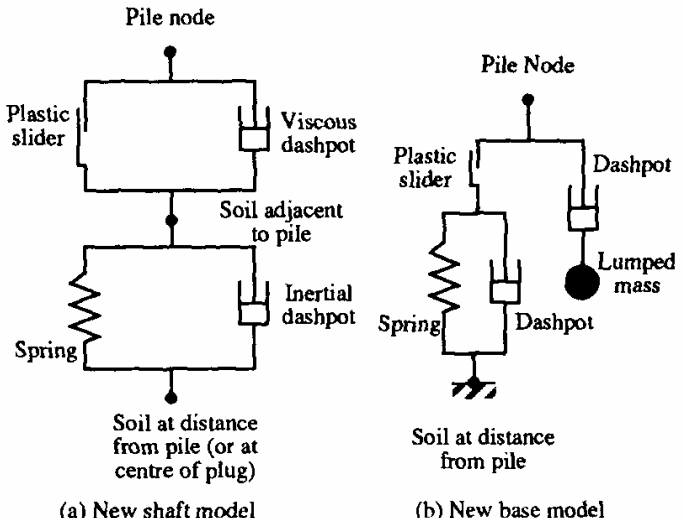

Figure 29: New shaft and base soil model.
(M.F. Randolph & A.J. Deeks – 1992)

2-2) Soil parameters:

Parameters requires for the soil models as describe above are springs stiffness (k), damping factors (C) and ultimate static or total resistances (R_u) of slider. Generally, these parameters are interpolated with ultimate resistance (R_u) or yielding value (F_{uy}) or soil shear modulus (G); quake value (q) and a supposed relation between static and damping resistance in order to reduce the variables in iterative procedure. The uses of those depend on researchers.

- Smith's model:

In the Smith's model the ultimate static soil resistance (R_u); quake value (q) and damping factor (J) are used to describe the soil behavior. As beginning input in the model, these values are estimated or empirical taken. The ultimate static resistance (R_u) is taken as the static capacity of the pile derived from soil profile. Hence, the shaft spring and toe spring given:

$$k_s = \frac{R_{ushaft}}{n.q_{shaft}} \qquad \text{and} \qquad k_{toe} = \frac{R_{utoe}}{q_{toe}}$$

where n is number of elements along the pile;

Quake value (q) is defined as the maximum elastic deformation of the soil. This is an empirical value and often taken as 2.5 mm for both shaft value (q_{shaft}) and toe value (q_{toe}).

$\delta < q \qquad R_s = K.\ \delta_{(t)}$

$\delta > q \qquad R_s = R_u$

$\delta_{(t)}$: displecement at time t.

The relation between static and dynamic resistance is supposed in the form:

$$R_{tot} = R_s.(1+J.v)$$

Where the damping constant J is empirically taken in the range of 0.05 – 0.5 s/m.

- In Mitwally et al, (1988) model, the soil parameters were determined from conventional soil investigation and laboratory test. The soil resistance is modeled using vertical plane strain soil reactions. The total soil resistance at the pile shaft is given by:

$\delta < q \qquad R_{s\text{-}total} = (G.S_1).\ \delta + (G.S_2/\omega).\ V$

$\delta > q \qquad R_{s\text{-}total} = (G.S_1).\ Q + (G.S_2/\omega).\ V$

and at the pile toe:

$\delta < q \qquad R_{t\text{-}total} = (G_t.r_o.C_1).\ \delta + (G_t.r_o.C_2/\omega).\ V$

$\delta > q \qquad R_{t\text{-}total} = (G_t.r_o.C_1).\ Q + (G_t.r_o.C_2/\omega).\ V$

where:

G, G_1 : shear modulus of the soil around pile shaft and below pile toe.

S, S_1, C, C_1 : dimensionless parameters represent stiffness and damping of the soil around pile shaft and below pile toe. S and S_1 are functions of the dimensionless frequency $a_o = r_o \omega/V_s$ and determined from vertical plane strain soil reactions calculation. C and C_1 are functions of the dimensionless frequency a_o and Poisson's ratio ν and determined in the same way as S and S_1 (*Mitwally et al, 1988*).

Q : "quake" value, equals to 2.5mm

r_0 : pile radius.

ω : the cicular frequency of the excited force.

- In Randolph et al, (1992) model, soil parameters are estimated from shear modulus (G) and Poisson's ratio (ν) as:

For the pile shaft: $k_s = \dfrac{0.75G}{(p\,d)}$ and $c_r = \dfrac{G}{V_s}$

For the pile toe: $k_t = 2.G.d/(1-\nu)$ and $C_b = 0{,}8\,.\,d^2.\sqrt{G\rho}\,/(1-\nu)$ for both dashpots

Lumped mass at pile toe: $M_b = 2.d^3.\rho.(0{,}1-\nu^4)/(1-\nu)$

The ultimate soil resistance (R_u) is taken as total dynamic soil resistance (R_{tot}) and the relation between static and damping resistance is:

$$R_{toy} = R_s.\left[\,1+\alpha.\left(\frac{\Delta v}{v_o}\right)^{\beta}\,\right]$$

where :

v_0 : a reference velocity (conveniently taken as 1).

Δv : the relative velocity between the pile and adjacent soil.

α, β : parameters, which are suggested by Gibson and Coyle (1968), Heerema (1979), Litkouhi and Poskitt (1980) as $\beta = 0.2$ and α varying from about 0.1 for sand to 1 for clay.

3.3.2. Finite element analysis

The first application of Finite element analysis (FEM) to pile driveability was proposed by Chow and Smith (1982) in order to overcome some limitations of the one-dimensional wave analysis associated with offshore foundations. The analysis procedure is similar to that described in Quasi-static test. Recent studies have proved that the results of dynamic pile tests can be evaluated using a FEM analysis (Kirsch et al, 2000); and the potential of a FEM coupled with dynamic formulation to the excess of pore water pressure under dynamic axial loads (Pinto, 2000).

3.3.3. Case history

This case history presents:

- The applicability of dynamic testing method to difference kinds of pile.
- The potential applicability of FEM in evaluating the test result as well as considering the local effects due to difference construction stages.

Dynamic pile load tests and finite element calculations for the bearing capacity of a quay wall foundation – container terminal Altenwerder, Port of Hamburg (Kirsch et al, 2000).

The construction of new quay wall in the port of Hamburg started in April 1999. The soil profile, pile details and test program described clearly in the reference. Dynamic pile load tests were performed in order to proof the bearing capacity of the foundation. Static pile load tests were also performed for the purpose of comparison, one of which was done with an instrumented pile to allow skin friction and end bearing to be evaluated separately. All dynamic test results were obtained by the CAPWAP procedure. The set-up effects are also

checked by performing restrike tests. Special questions called for detailed FEM analysis of the load – displacement behavior of single piles in certain construction stages.

Figure 30 shows an overview of the load calculated capacities split into skin friction and toe bearing. Figure 31 shows the typical load displacement curve calculated by CAPWAP and measured from static test. The testing results revealed a significant reduction in the bearing capacity of all pile in the construction area. It was explained by the fact that the bottom soil layer (boulder clay), in which the piles embedded, is softer than the soil investigated result (Kirsch et al, 2000). To solve the problem, the re-design of the piles was performed, i.e. extended the concrete pile's length; changed the designed of steel piles by trying different pile shoes with wings and filling sheets. It demonstrated that fast performance and relatively low cost of Dynamic pile load test made optimization for the pile foundation design.

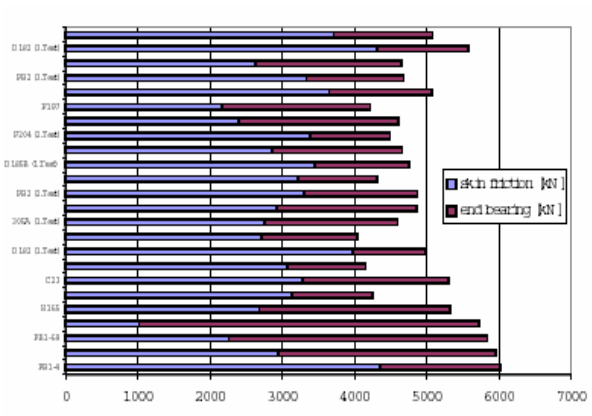

Fig 30: CAPWAP results of pile capacities. (Kirsch et al, 2000)

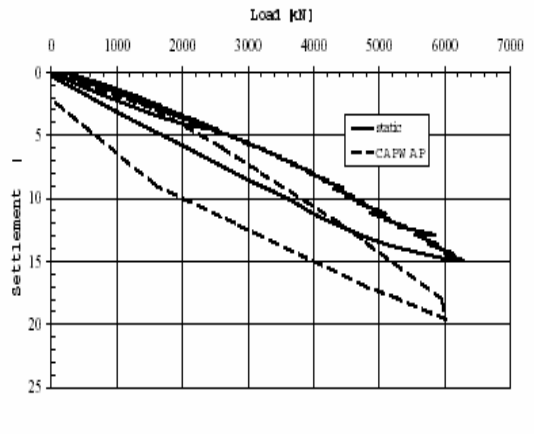

Fig 31: Typical load-displasement of concrete pile (Kirsch et al, 2000).

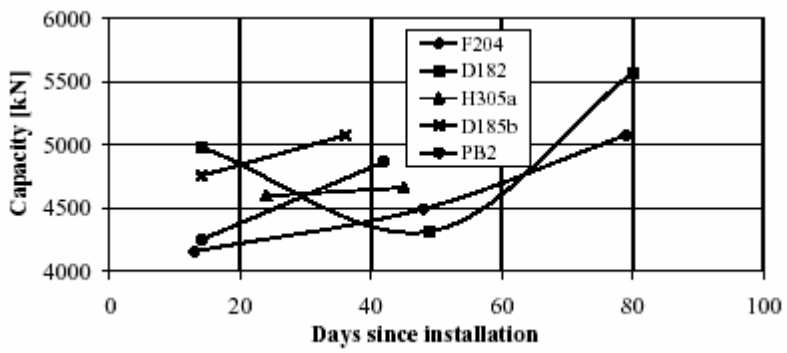

Figure 32: Set-up of the driven cast-in-place piles.

Figure 32 shows the set-up effects of driven cast-in-place piles. Generally, the gain in bearing capacity is 10% to 20% within two month after installed. The reduction and subsequent regain in capacity of pile D182 was object of FEM analysis.

The FEM analysis was performed in pile D182 in order to proof that the reduction is not because of a general loss of strength of the surrounding soil but because of the disturbance of the ground adjacent due to the recent cutting of the slurry trench. The pile D182, the slurry trench, and adjacent soil are modeled in 3D FEM analysis in figure 33. The finite element mesh consisted of a total 1988 second order shape function brick elements. Two diference cases were investigated and the findings were compared with the results of two dynamic tests in the same case. One is performed before and one is after the cutting of the slurry trench. Result of pile load-displacement curve in figure 34. The result proved that the FEM analysis can bearing capacity from dynamic tests and allowed the explaination of local effects due to

different construction stages. The reduction in the bearing capacity is possibly caused by the installation of the slurry trench.

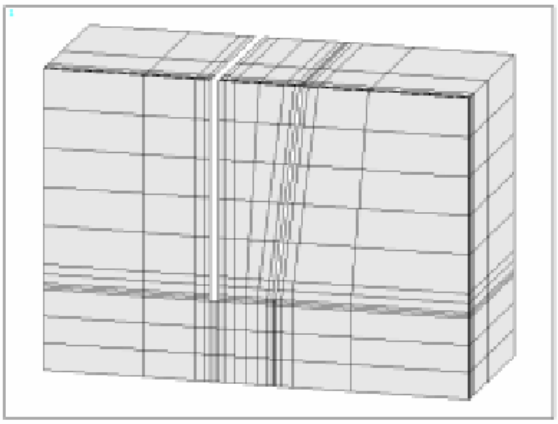

Fig. 33: 3D FE mesh for pile D182 with adjacent trench (Kirsch et al, 2000).

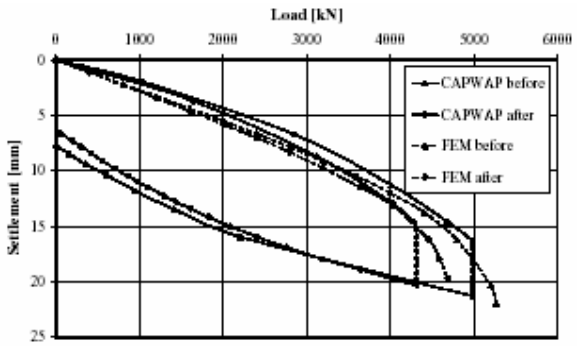

Fig. 34: Load-displacement curves of pile D182 (Kirsch et al, 2000).

IV. Some problems with the non – static test results

The above presentations give an overview about dynamic and quasi – static pile load test. Available interpretation methods, such as one – dimensional stress-wave theory or dynamic finite element method are capable to evaluate the capacity and static load – displacement of pile. However, these interpretation methods have limitations in their applications in practice because the soil models and soil parameters used in these interpretation methods not clearly and fully described all pile - soil system behaviors during the tests as in – situ observed. For instance, the excess of pore pressure during the tests and the damping model for the rate effect as introduced below.

4.1. Excess pore pressure

Table 3: Summary of pore pressure measurement casehistories

Reference	Soil type	Pile type	Collected data
P. Holscher (1992)	sand	Pre-fabricated reinforced concrete	Excess pore pressure at last blow of driving, during dynamic and STATNAMIC test
Eiksund et al. (1996)	Sand and silt	Model closed-ended steel pile	Velocity dependency resistance and excess pore pressure at pile toe
Matsumoto (1995, 1998)	Diatomaceous mudstone	Open-ended pipe pile	Excess pore pressure, soil resistance during static, dynamic and STATNAMIC test
Maeda et al. (1998)	Gravel sand	Cast-in-place concrete pile	Excess pore pressure, soil resistance during STATNAMIC test

Measuring the excess pore pressure during pile driving and non – static pile load tests is object of many researchers. The results show that the build – up and dissipation of excess pore pressure is correlative to loading duration; the excess pore pressure may be positive or negative. The observations of excess pore pressure, soil deformations during and following

pile driving around closed – ended pile in clay is summarized by Pestana et al. (2002) then added by Gupta (2003). The other similar works are done by Benamar (2000) on model steel pile in clay; Jin – Hung Hwang et al. (2001) on driven precast concrete pile in layered soil in Taiwan. The observations during pile load tests such as Holscher (1992), Eiksund et al. (1996), Matsumoto (1995, 1998), and Maeda et al. (1998) are of interested and presented here (table3).1) P. Hölscher (1992) measured the excess pore pressure during pile driving, dynamic test and quasi – static test for the pre – fabricated reinforced concrete pile embedded 3,2m in sand layer with the depth of pile toe of 18,2m in Delft – The Netherlands. The results of excess pore pressure for the last blow of driving, the dynamic test 3 days later and the quasi – static test 5 days later in figure 35. It shows a large pore water pressure occurred during the non – static tests and the consolidation time of soil around the pile toe is relatively long in relation to the quasi – static loading time (between 100ms and 200ms). Therefore, the effective stress may be changed, as result the static capacity of the pile may be affected.

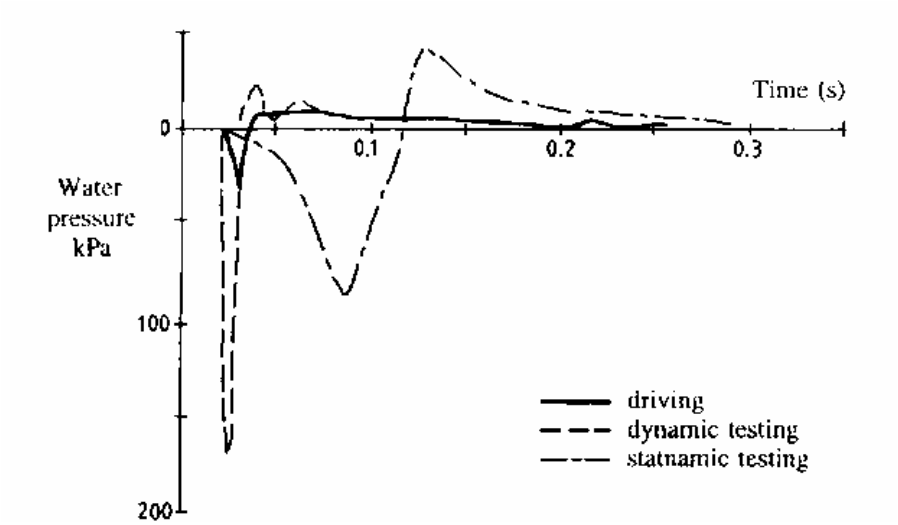

Figure 35: Pore pressure during pile driving, dynamic and quasi-static tests (Holscher, 1992).

2) Eiksund et al. (1996) presented the results from a model pile test program aimed to study dynamic soil resistance and excess pore pressure near the pile toe during dynamic tests. The model pile was a closed end steel tube with length 1,07m; 63,5mm in diameter. The model pile was driven with penetration velocities ranging from 0,8 to 1800mm/s in cubical pressure chamber of 1m3, which filled with F-75 Ottawa sand or Lebanon silt. Typical pore pressure responses in sand and in silt are show in figure 36 and figure 37. The dense Ottawa sand showed a typical dilatant behavior with the negative pore pressure response that increase the dynamic resistance and the Lebanon silt showed the positive pore pressure response. The ratio between peak pore pressure force and dynamic force is about 0,2% for sand and 1,5% for silt.

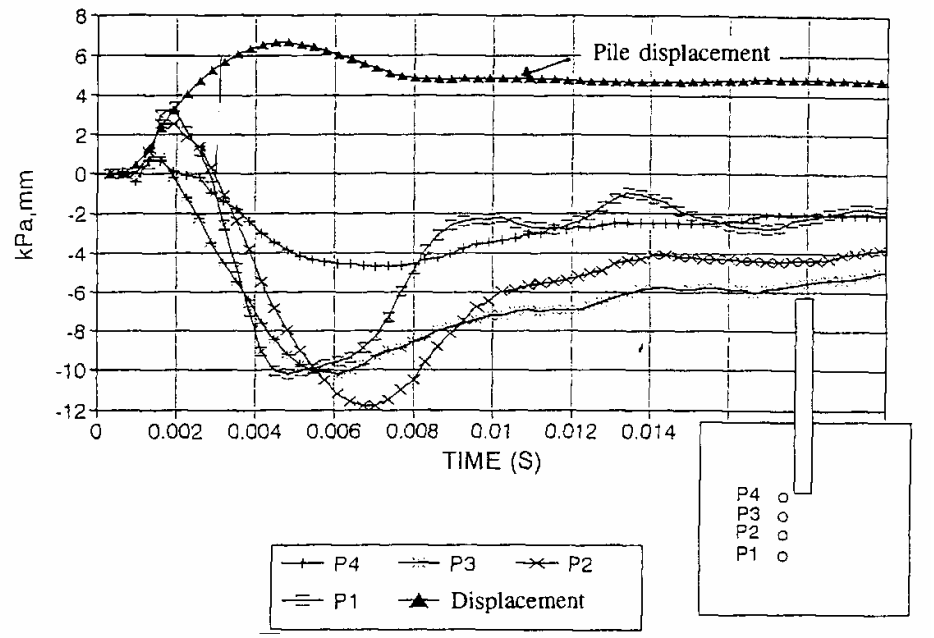

Figure 36: Typical pore pressure in Ottawa sand, 0,8m height (Eiksund et al. 1996).

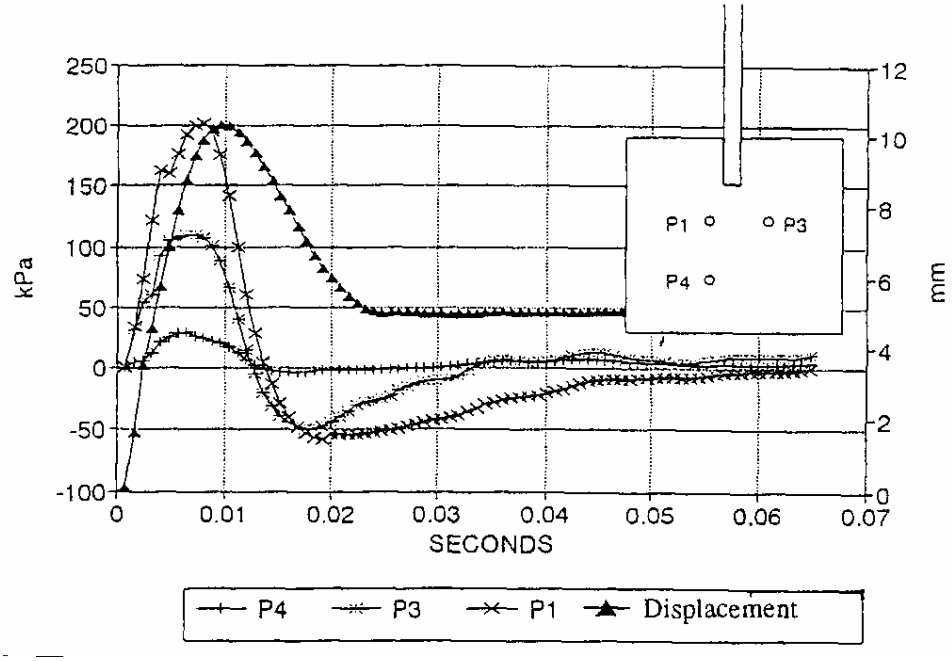

Figure 37: Typical pore pressure in Lebanon, 0,3m height (Eiksund et al. 1996).

3) Matsumoto (1995) measured the excess pore pressure during the dynamic test and cyclic static test on open – ended pipe pile in a diatomaceous mudstone (a kind of soft rock). He observed a large positive pore pressure built – up near the pile shaft and negative pore pressure built – up at relative far from pile shaft. This indicates the excess pore pressure is more complex than that modeling by theories of expansion of cylindrical cavity under undrained and plane strain conditions, which widely used.

Matsumoto (1998) measured the excess pore pressure during the STATNAMIC test in the same pile, then analysis the results by FEM. He also observed a large pore pressure built – up and dissipation in the time between 100ms and 200ms. The pore pressure generated is negative at pile shaft and positive near pile toe. Also the ratio between peak pore pressure force and dynamic force is about 0,2% for this case. His measurements and FEM analysis

results are showed in figure 38. The figure also shows the difference between the undrained and drained analysis condition (the shaft capacity in undrained condition is smaller than that in drained condition) and the existence of dynamic effect in the STATNAMIC test (compare between the load – displacement from STATNAMIC and static test). The excess pore pressure analysis is comparable with measured result at pile toe but shown all positive excess pore pressure at pile shaft. Comparison between calculated and measured static load – displacement shows the bigger capacity in calculated curve. It might be related to the set – up effect (because the STATNAMIC test was performed 14 months after the static test) or the limitation of linear elastic soil model or other unknown effects, which need more research.

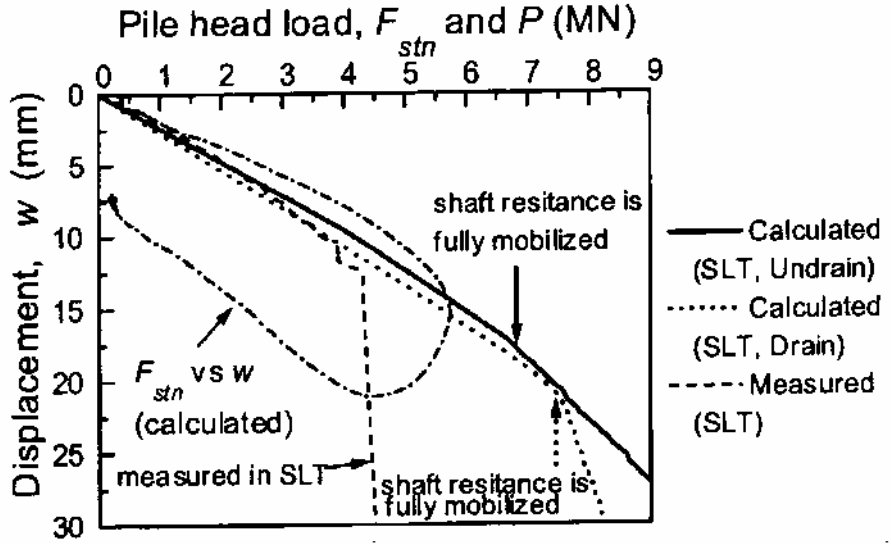

Figure 38: Measured and calculated results of Matsumoto (1998).

4) Maeda et al. (1998 – case history 2 – part II) measured the excess pore pressure during the STATNAMIC test on cast – in – place concrete pile embedded 1,2m in gravel sand. His result in duration of pore pressure is the seem as Matsumoto's but the resistance ratio is about 0,6%.

All above case studies especially the analysis of Matsumoto (1998) show the behavior of the soil during the non – static and static test is far difference even between the static behaviors derived from the dynamic one in drained and undrained condition. Simple compare the effect of pore pressure response by the ratio between pore pressure force (by simple multiple the excess pore pressure by pile area) and dynamic force show small effect. But considering the response condition between non – static tests and static test its effect have to be taken into account in order to derive a static load – displacement behavior of the pile under the drained condition. This problem is not cleared at this moment.

4.2. Loading rate effect

It's known that the shear strength of soil depends on the rate of loading but how the pile capacity depends on rate of loading during the pile load test is not clear until now, although it was implied by damping factor as usually use in wave equation analysis. While the rate effect in clayey soil has long been confirmed and well summarized by *Hyde et al. (1998),* the rate effect in sandy soil is not clearly defined. The results of 11 test cases in sandy soil from Japanese Research Committee on Rapid Pile Load Test Methods show the ratio between maximum STATNAMIC load and static load at the same displacement of maximum STATNAMIC load ranges from 1.12 to 1.96 (*table 4 – Kusakabe, 1998*). This implies an obviously increasing in STATNAMIC load compare to static load in sandy soil and the increasing may reach 100%. It should be remarked that the usage of maximum F_{soil} (derived from STATNAMIC force minus inertial force) for above ratio is more adequate but unfortunately, the acceleration records is not available. On the other hand, laboratory soil tests on sandy soil show different trend, i.e. increase, decrease and no rate effect as presented here.

4.2.1. Rate effect laboratory tests:

Many researchers have long interested the time – dependent behavior of sand. ***Casagrande & Shannon (1948)*** performed triaxial compression tests on dry Manchester sand. The sand samples were 7.1cm in diameter and 18cm in height; the void ratio at densest was 0.61 and at loosest id 0.88. The confining pressures were from 30 to 90 kPa; the loading velocity up to 0.2 m/sec. Their conclusion was the strength of dry sand increases about 10 to 15% from 10 minutes static tests when tested at high loading rates. ***Seed & Lundgren (1954)*** performed drained and undrained triaxial tests on saturated sands at confining pressure of 200 kPa and loading velocity up to 1 m/sec. They observed that during transient drained testing, the pore pressure had insufficient time to drain so the tests approached undrained conditions. They concluded that the increasing in strength of dense saturated sand was from 10 to 15% due to the effect of rate of loading; the effect of rate of loading decrease as void ratio increase; and the loose saturated fine sand may be decrease in strength with the increasing of loading rate. ***Whitman & Healy (1962)*** presented the results of drained and undrained triaxial tests on dense and loose sands with confining pressure of 70 kPa and loading velocity up to 0.5 m/sec. The results indicated 10% increased in drained strength and up to 100% increased in undrained strength over static values (failure time was 5 min.). ***Lee & Seed & Dunlop (1969)*** performed compression triaxial tests on dense and loose sand with various confining pressure from 100 to 1475 kPa; loading velocity up to 0.22 m/sec. Their findings were 7% increase in strength of loose sand with increase of loading velocity in all confining pressure; and up to 20% for dense sand in high confining pressure. Most recently, Yamamuro & Abrantes (2003) show the results of drained triaxial compression tests on loose crushed coral sand at the strain rate from 0.0022 %/s to 1500 %/s at 98 kPa and 350 kPa confining pressure. Their findings are the increasing in deviator stress up to 30% and secant modulus up to 115% as the strain rate increase. The summary is given in table 4.

Table 4: Summary of laboratory rate effect tests on sand

Authors	Test type	Sand samples	Results
Casagrande & Shannon (1948)	Vacuum triaxial compression	Dry Manchester sand	10% increase in strength
Seed & Lundgren (1954)	Drained and undrained triaxial tests	- Dense saturated - Loose saturated	- 15-20% increase - may be decreased
Whitman & Healy (1962)	Drained and undrained triaxial tests	- Dense saturated - Loose saturated	- 10% increase in drained strength - 100% increase in undrained strength
Schimming, Haas & Saxe (1966)	Direct shear test	Dry sand	Almost no loading rate effect
Lee, Seed & Dunlop (1969)	Triaxial compression	Loose dry Dense dry	7% increase up to 20% increase
Yamamure & Abrantes (2003)	Drained triaxial compression	Loose dry	- Up to 30% increase in peak stress. - Up to 115 % increase in secant modulus.

4.2.2. Rate effect from other tests:

Jezequel (1969) pushed an electric cone penetrometer in medium dense sand at rate of penetration from 0.2 cm/sec to 2 cm/sec. His results showed the resistance increased 8% above the water table and decreased 21% under the water table. ***Brumund et al. (1973)*** used shear box test to measure the static and dynamic friction between sand and typical construction material. The loading time was 1-2 msec and 5 min.; the loading rate was from 5.10^{5} to 0.5 psi/min. Their results showed the dynamic wall friction was greater than that of static about 20%. ***Dayal & Allen (1974)*** used an instrumented impact cone penetrometer to measure the

cone and sleeve resistance of loose and dense sand sample at difference penetration rate (from 0.13 cm/sec to 81.14 cm/sec). They concluded that the effects of penetration velocity on cone and sleeve resistances are insignificant for granular soil. ***Heerema (1979)*** performed a simple laboratory test simulating the action of steel pile wall in the soil during driving in order to determine the relationships between wall friction, horizontal stress and pile wall velocity. His results on sand showed the friction force was linearly dependent on normal stress and independent of velocity. Recently, model pile tests on sand with difference loading velocities have performed. ***Al – Mhaidib (1999)*** performed 45 compressive capacity tests on model pile embedded in sand with loading velocity from 0.01 mm/min to 1mm/min. His results showed the increase in capacity with the increase of loading rate. ***Gennaro et al. (…..)*** studied the effects of loading rate on pile resistance by performed a series of model pile tests in calibrated sand chamber. Their results showed significant effect of loading rate on side resistance and insignificant effect to point resistance. One interested point in their results was the strongly decrease of side resistance with increase of loading rate.

V. Conclusion and recommendation:

The paper has summarized the quasi – static and dynamic pile load test methods with state–of–the–art in testing procedures and interpretation methods as well as some remain problems related to interpretation methods with concentrating in STATNAMIC test. The available interpretation methods, these non – static pile load tests have proved an economic testing method to evaluate the static capacity and load – displacement of a pile. The case histories make clear the economy and applicability of the non – static tests. The dynamic FEM analysis seems to be the best interpretation method particularly the capacity in modeling the pile behaviors. But there still some problems are remaining in the interpretation procedures. It lies in the dynamic effects taken into account such as the effect of excess pore pressure and the loading rate affect. Further study should be clarified following problems:

- The effect of pore pressure for any soil type should be made clear in order to derive the uniqueness load – displacement behavior of the pile.
- The quantity loading rate affects should be figured out in every particular case from fundamental soil tests and its correlation to damping factor used in stress-wave analysis.
- Finally, how exactly of the taking of all dynamic forces during the test as velocity dependency as usual in stress-wave analysis or we should put some other coefficients for all the effects instead of only damping factor J.

References

Brown, D.A., 1994. *Evaluation of static capacity of deep foundations from STATNAMIC testing*, Geotechnical testing journal, Vol. 17, No. 4, pp. 403-414.

Bermingham, P. & Janes, M.C. 1989. An *innovative approach to load testing of high capacity piles*, Proc. of Int. Conf. on piling and deep foundation, pp. 409-413.

Ealy, C.D. & Justason, M.D. 1998. *STATNAMIC and static load testing of a model pile group in sand*, Proc. 2 nd Int. STATNAMIC seminar, Tokyo: 169-178.

Eiksund, G. & Nordal, S., 1996. *Dynamic model pile testing with pore pressure measurements*, Proc. 5 nd Int. Conf. Application of stress-wave theory to piles, Florida: 581-588.

El Naggar, M.H., Novak, M. 1992. *Analytical model for an innovative pile test*. Canadian geotechnical journal, 29: 569-579.

El Naggar, M.H., Baldinelli, M. 1998. *Stress wave analysis of STATNAMIC load test for bearing capacity prediction*, Proc. 2 nd Int. STATNAMIC seminar, Tokyo: 327-335.

Goble, G.G., et al., 1980. *The analysis of pile driving – A state-of-the-art*. Proc. 1st Int. Conf. Application of stress-wave theory to piles, Stockholm: 331-362.

Goble, G.G., et al., 1995. *Discussion on "Evaluation of static capacity of deep foundations from STATNAMIC testing" by Dan Brown*, Geotechnical testing journal, Vol. 18, No. 4, pp. 493-498.

Gonin, H., Coelus, G. & Leonard, M. 1984. *Theory and performance of a new dynamic method of pile testing*, Proc. 2nd Int. Conf. Application of stress-wave theory to piles, Stockholm: 403-410.

Horikoshi, K., Kato, K. & Matsumoto, T. 1998. *Finite element analysis of STATNAMIC loading test of pile*. Proc. 2 nd Int. STATNAMIC seminar, Tokyo: 295-302.

Holeyman, A.E. 1992. *Keynote lecture: Technology of pile dynamic testing*, Proc. 4 nd Int. Conf. Application of stress-wave theory to piles, The Hague: 195-216.

Janes, M.C., Bermingham, P.D. & Horvath, R.C. 1991. *An innovative dynamic test method for piles*, Proc. 2nd Int. Conf. Recent advances in geotechnical earthquake engineering and soil dynamics, St. Louis, Missouri, Paper No. 2.20

Janes, M.C., Sy, A., Campanella, R., 1994. *A comparison of STATNAMIC and static load tests on steel pipe piles in the Fraser Delta*, Proc. 8st annual symposium on deep foundations, Vancuver.

Janes, M.C., Justason, M.D. & Brown, D.A. 1998. *Proposed ASTM Standard test for piles under rapid axial compressive load with its draft paper " Long period dynamic load testing ASTM Standard draft " presented to the seminar for technical disscussion*, Proc. 2 nd Int. STATNAMIC seminar, Tokyo: 199-118.

Justason, M.D. et al. 1998. *A comparison of static and STATNAMIC load tests in sand: A case study of the Bayou Chico bridge in Pensacola, Florida*, Proc. 2 nd Int. STATNAMIC seminar, Tokyo: 43-53.

Kato, K., Horikoshi, K. & Matsumoto, T. 1998. *Analysis of STATNAMIC load tests by using a new single mass model*. Proc. 2 nd Int. STATNAMIC seminar, Tokyo: 273-278.

Maeda, Y., et al., 1998. Applicability of unloading-point-method and signal matching analysis on the STATNAMIC test for cast-in-place pile. Proc. 2 nd Int. STATNAMIC seminar, Tokyo: 99-108.

Mc. Vay, M., et al. 2003. *Final report: Calibrating resistance factors for load and resistance factor design for STATNAMIC testing.*

Middendorp, P., Bermingham, P.D. & Kuiper, B. 1992. *STATNAMIC load testing of foundation piles*, Proc. 4 nd Int. Conf. Application of stress-wave theory to piles, The Hague: 581-588.

Middendorp, P. & Bielefeld, M.W. 1995. *STATNAMIC load testing and the influence of stress wave phenomena*, Proc. 1 st Int. STATNAMIC seminar, Vancouver: 207-220.

Middendorp, P. & van Foeken, R.J. 1998. *When to apply dynamic load testing and STATNAMIC testing*, Proc. 2 nd Int. STATNAMIC seminar, Tokyo: 253-261.

Middendorp, P. 2000. *Keynote leture: STATNAMIC the engineering of art*. Proc. 6 nd Int. Conf. Application of stress-wave theory to piles, Sao Paolo: 551-562.

Pinto, P.L. 2000. Modelling pore pressure generation during testing of deep foundations. Proc. 6 nd Int. Conf. Application of stress-wave theory to piles, Sao Paolo: 275-278.

Poulos, H.G. 1998. *Keynote lecture: Pile testing-From the designer's viewpoint*, Proc. 2 nd Int. STATNAMIC seminar, Tokyo: 3-21.

Randolph, M.F. & Deeks, A.D. Keynote lecture: Dynamic and static soil models for axial pile response, Proc. 4 nd Int. Conf. Application of stress-wave theory to piles, The Hague: 3-14.

Schellingerhout, A.J.G. & Revoort, E. 1996. *Pseudo static pile load tester*, Proc. 5th Int. Conf. Application of stress-wave theory to piles, Florida: ???

Smith, A.E.L. 1962. *Pile-driving analysis by wave equation*. ASCE, Journal of soil mechanics and foundation division, Vol. 127, No. 1, pp. 1145-

APPENDIX A

The basis one – dimensional wave equation: $u(x,t)_{tt} = c^2 . u(x,t)_{xx}$ (1)

The characteristic solution for equation 1 given:

$$u = f(x-ct) + g(x+ct) = u\downarrow + u\uparrow \quad (2)$$

Differentiation equation 2 to time t and position x given the upward and downward velocity and force waves:

$$V = V\downarrow + V\uparrow = -c .u'\downarrow + c .u'\uparrow \; ; \quad F = -E.A.\frac{\partial u}{\partial x} = F\downarrow + F\uparrow = -EA.(u'\downarrow + u'\uparrow)$$

Where: $V\downarrow = -c .u'\downarrow$; $F\downarrow = -E.A.u'\downarrow = \frac{A.E}{c} . c.u'\downarrow = Z.u'\downarrow$ (3)

$V\uparrow = c.u'\uparrow$; $F\uparrow = -E.A.u'\uparrow = - \frac{A.E}{c} . c.u'\uparrow = - Z.u'\uparrow$ (4)

Combine equation (3) & (4) given:

$$F = F\downarrow + F\uparrow = Z.(V\downarrow - V\uparrow) \quad \text{and} \quad V = \frac{1}{Z} .(F\downarrow - F\uparrow) \quad (5)$$

$$F\uparrow = \frac{F - Z.V}{2} \quad \text{and} \quad F\downarrow = \frac{F + Z.V}{2} \quad (6)$$

Now, we consider a propagation of an impact wave along a pile shaft, where soil resistance appears. The soil resistance is assumed to concentrate at point m in pile shaft and at pile toe (figure a-1). Four time periods will be considered. The measured items at pile head are force F(0,t) and velocity V(0,t) as function of time.

- $0 \le t_1 < m/c$

The wave introduces at pile head (x = 0) at time $t_0 = 0$ and propagates undisturbed downward along the pile.

$F(0,t_1) = F(t_1)\downarrow + F(t_1)\uparrow$ and $V(0, t_1) = V(t_1)\downarrow + V(t_1)\uparrow$

Because of no friction, there is no upward traveling wave, i.e. $F(t_1)\uparrow = 0$ and $V(t_1)\uparrow = 0$.

- $m/c \le t_2 < L/c$

The downward wave meets the shaft resistance W, the wave will partly transmit and reflect. The equilibrium condition: $F_1(m,t_1 + m/x) = W + F_2(m,t_1 + m/x)$

The continuity condition: $V_1(m,t_1 + m/x) = V_2(m,t_1 + m/x)$

These conditions given:

$F_1(m,t_1 + m/x)\uparrow = F_2(m,t_1 + m/x)\uparrow + 1/2 . W$

$F_2(m,t_1 + m/x)\downarrow = F_1(m,t_1 + m/x)\downarrow - 1/2 . W = F(0,t_1)\downarrow - ½ .W$

$V(m,t_2) = \frac{1}{Z} . F_2(m,t_1 + m/x)\downarrow = \frac{1}{Z} . (F(0,t_1)\downarrow - ½ .W)$

Because at the time ($t_2 = m/c$), $F_2(m,t_1 + m/x)\uparrow = 0$ so $F_1(m,t_1 + m/x)\uparrow = 1/2 .W$. It means that during the period ($m/c \le t_2 \le 2m/c$) the upward traveling force equal to half of the shaft resistance at point m. This wave will be seen at pile head at time t = 2m/c.

- $L/c \leq t_3 < (L+m)/c$

The downward wave $F_2(m,t_2)\downarrow$ arrives at pile toe and meets the toe resistance P. The conditions are F = P. Hence:

$$F_3(L,t_3)\uparrow = F_3(L,t_1 + L/x)\uparrow = P - F_2(m,t_2)\downarrow = P - F(0,t_1)\downarrow + \tfrac{1}{2}.W$$

$$V_{toe} = V(L,t_3) = \frac{1}{Z}.(2.F_2(m,t_2)\downarrow - P)$$

- $(L+m)/c \leq t_4 \leq 2L/c$

The upward wave $F_3(L,t_3)\uparrow$ arrives at point m, and partly transmit and reflect. Hence:

$$F_4(m,t_4)\uparrow = F_3(L,t_3)\uparrow + \tfrac{1}{2}.W = (P + W) - F(0,t_1)\downarrow \qquad (\ldots)$$

$$\text{or } F(0,t_1)\downarrow + F_4(m,t_4)\uparrow = (P + W) \qquad (a\text{-}\ldots)$$

The upward wave $F_4(m,t_4)\uparrow$ will travel undisturbed to the pile head at time (2L/c).

Equation (a-1) shows that the total soil resistance, i.e. the toe resistance (P) plus the shaft resistance (W), is equal to the downward traveling force at pile head at time (t_1) during the impact plus the upward traveling force at pile head at time ($t_2 = t_1 + 2L/c$).

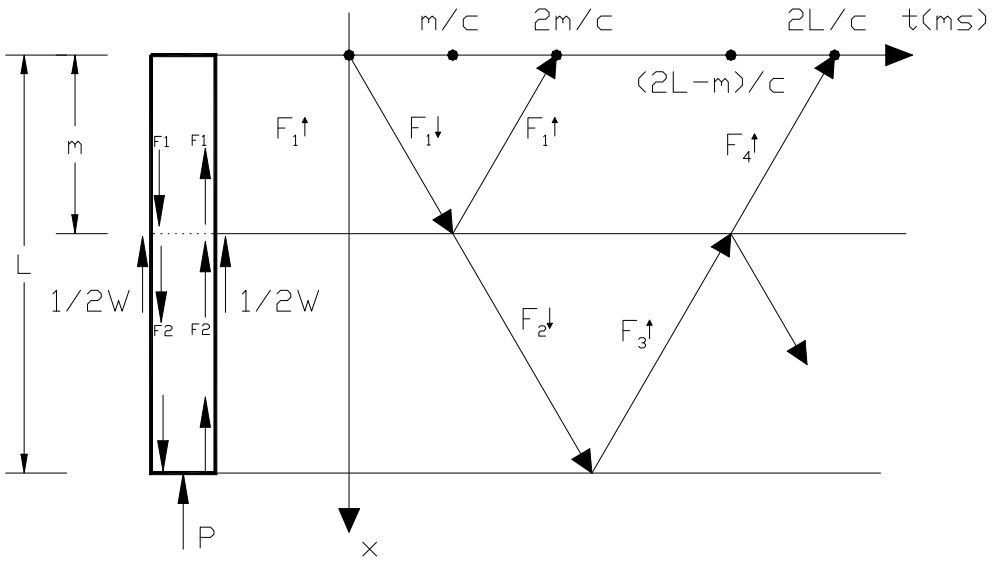

Figure 42: One wave propagation cycle in pile